

THE ROLE OF PRESSURISED WATER IN LARGE-SCALE GLACIOTECTONIC THRUSTING: MICROMORPHOLOGICAL EVIDENCE FROM THRUST-BLOCK MORAINES IN MELASVEIT, W-ICELAND

Thorbjörg Sigfúsdóttir[1,2], Emrys Phillips[3,4], Ívar Örn Benediktsson[2]

[1]Department of Geology, Lund University, Sölvegatan 12, 223 62 Lund, Sweden; [2]Institute of Earth Sciences, University of Iceland, Sturlugata 7, 101 Reykjavík, Iceland; [3]British Geological Survey, The Lyell Centre, Research Avenue, Edinburgh, EH14 4AP, UK; [4]Department of Geography, Queen Mary University of London, Mile End Road, London, E1 4NS, UK.

Corresponding author:

Thorbjörg Sigfúsdóttir. Institute of Earth Sciences, University of Iceland, Sturlugata 7, 101 Reykjavík, Iceland. Email: thorbjorg.sigfusdottir@geol.lu.se. Tel: 00 354 8467961

ABSTRACT

Pressurised meltwater enhances the ability of glacier to detach and transport large blocks of sediment /bedrock by minimising friction occurring along structural surfaces. However, a detailed understanding of these processes has yet to be established. This study focuses on micro-scale structures developed within décollements in two thrust-block moraines of Late Weichselian age in Melasveit, western Iceland. The aim is to investigate how detachments form in glaciotectonised sequences and how large sediment blocks/rafts can be dislocated and transported by glaciers. A model is proposed which argues that the introduction of pressurised water into weak beds (silt/sand) played a key role in the detachment and movement of the thrust-blocks. The deformation associated with their transport was focused within thin, water-lubricated zones allowing the unlithified and unfrozen sediment blocks to move without undergoing extensive internal disruption. The style of deformation changed temporally and spatially during the transport reflecting fluctuating water pressures within the detachments. Repeated events of hydrofracturing and water-escape caused the thrust-stack to drain, resulting in the progressive locking up of the detachments and eventual accretion of the thrust blocks. The model may be applicable to other similar thrust-block complexes as well as for processes occurring during glaciotectonic sediment rafting.

INTRODUCTION

Pressurised meltwater beneath glaciers and ice sheets is believed to have major effect on ice sheet dynamics as well as deformation and sedimentary processes (e.g. Boulton et al., 1974; Boulton and Caban, 1995; Hiemstra and van der Meer, 1997; Rijsdijk et al., 1999; van der Meer et al., 2009; Phillips and Auton, 2000; Boulton et al., 2001; Khatwa and Tulaczyk, 2001; Baroni and Fasano, 2006; Phillips et al., 2007; Sole et al., 2011; Moon et al., 2014). Increased porewater pressures can cause accelerated flow (basal sliding) due to decoupling between the ice and its bed, as well as enhanced sediment remobilisation and deformation due to reduced sediment shear strength (e.g. Piotrowski and Tulaczyk, 1999; Boulton et al., 2001; Fischer and Clarke, 2001; Phillips et al., 2013a; Phillips et al., 2018; Evans, 2018). Deformation influenced by elevated water pressures can either result in the pervasive weakening of the sediment pile, or be focused along discreet, water-lubricated detachments (Alley, 1989; Fischer and Clarke, 2001; Kjær et al., 2006; Phillips and Merritt, 2008). The development of such low-friction detachments/décollements is thought to have a considerable effect on the style and magnitude of glaciotectonics facilitating the transport of large thrust-blocks of sediment and/or bedrock (Phillips and Merritt, 2008; Burke et al., 2009; Vaughan-Hirsch et al., 2013; Aber and Ber, 2007; Andreassen et al., 2007; Rüther et al., 2013) leading to the construction of large thrust-block or composite moraines (Croot, 1987; Bennett, 2001; Pedersen, 2005; Aber and Ber 2007; Benediktsson et al., 2008; Vaughan-Hirsch and Phillips, 2017; Phillips et al., 2017; Sigfúsdóttir et al., 2018).

It has been argued that the presence of a well-developed permafrost layer in front of the advancing glacier above the detachments can aid in the construction of large thrust-block moraines as it allows stress to be transmitted far into the forefield of the advancing glacier margin (Aber et al., 1989; Evans and England, 1991; Boulton and Caban, 1995; Boulton et al., 1999; Bennett, 2001; Burke et al., 2008) or the base of the frozen layer acts as a focus for detachment above which deformation occurs (Burke et al., 2008; Benediktsson et al., 2015).

Furthermore, it has been argued that the freezing of sediments and/or bedrock to the base of the glacier is important for transportation of detached, largely intact thrust-blocks (or rafts/megablocks) (Banham, 1975; Aber, 1988; Clayton and Moran, 1974; Bluemle and Clayton, 1984; Ruszczynska-Szenajch, 1987). However, it has increasingly been shown that overpressurised water within the substratum can cause the detachment and emplacement of large, unconsolidated thrust-blocks without the ground being frozen (Moran et al., 1980; van der Wateren, 1985; Broster and Seaman, 1991; Aber and Ber, 2007; Benn and Evans, 2010; Benediktsson et al., 2008; Phillips and Merritt, 2008; Vaugh-Hirsch and Phillips, 2017; Phillips et al., 2017). Such sediment blocks can be transported over long distances; for example, thrust-bound rafts of glaciomarine sediments in Clava, Scotland, were shown to have been transported subglacially at least 50 km from their origin aided by the fluid flow along the décollement surfaces (Phillips and Merritt, 2008).

However, a detailed understanding of the processes occurring along the major detachments formed during glaciotectonism has yet to be established. This paper addresses this lack of understanding and presents the results of a detailed micro-and macroscale investigation of the detachments developed within two glaciotectonic complexes in Melasveit, western Iceland. These complexes are composed of subhorizontal thrust-blocks (nappes) of unlithified marine sediments and were formed during an active retreat of a marine-terminating glacier emanating from Borgarfjörður in the Late Weichselian (Fig.1; Ingólfsson 1987, 1988; Sigfúsdóttir et al., 2018). As these thrust-block moraines were formed in a submarine environment, it can be assumed that the sediments were unfrozen at the time of deformation. This study uses micromorphology to investigate the factors controlling the changing style of deformation which occurred during the detachment, transport and emplacement of the thrust-blocks; in particular, the effect of the introduction of pressurised water along the bounding thrusts during this process. The results of this microstructural study are discussed in the wider context of the interrelationships between the glacier dynamics, submarginal hydrology and glaciotectonics.

Location of the study area and its geological context

The Melasveit district of western Iceland is a coastal lowland area situated between the fjords of Borgarfjörður and Hvalfjörður (Fig. 1a). The geology of the area is dominated by a >30 m thick sequence of Late Weichselian to Holocene glaciomarine to deltaic sediments overlying striated bedrock surface (Ingólfsson, 1987, 1988; Sigfúsdóttir et al., 2018). The bedrock in the Melasveit area is mainly composed of Neogene basaltic lava flows which are thought to have largely originated from the extinct Hafnarfjall-Skarðsheiði central volcano located to the north-east (Franzson, 1978).

Like most coastal areas in Iceland, the Melasveit district was covered by ice during the Last Glacial Maximum (LGM). The area subsequently deglaciated rapidly between c. 15-14.7 cal. ka BP, following the collapse of the marine-based western sector of the Icelandic Ice Sheet (IIS) (Ingólfsson, 1987, 1988; Syvitski et al., 1999; Jennings et al., 2000; Norðdahl et al., 2008¸ Ingólfsson et al., 2010; Norðdahl and Ingólfsson, 2015; Patton et al., 2017). Immediately following the deglaciation of Melasveit, the relative sea level in surrounding regions was 125-150 m higher than present (Ingólfsson and Norðdahl, 2001; Norðdahl and Ingólfsson, 2015). Consequently, this low-lying area remained below sea level throughout most of the Late Weichselian leading to the deposition of a thick sequence of glaciomarine sediments.

The relative sea level fluctuated considerably during this time, reaching a maximum during a phase of renewed glacier expansion in both the Younger Dryas (*c*. 12.7-11.7 cal. ka BP) and Early Preboreal (*c.* 11.7-10.1 cal. ka BP) when the sea levels were 60-70 m higher than present (Ingólfsson, 1988; Norðdahl et al., 2008; Ingólfsson et al., 2010).

After the initial deglaciation of Melasveit during the Bølling chronozone, the IIS re-advanced from the north while the area was still isostatically depressed and culminated with the construction of the Skorholtsmelar end-moraine (Fig. 1b) (Ingólfsson 1987, 1988; Ingólfsson et al., 2010; Sigfúsdóttir et al., 2018). The active retreat of the marine-terminating glacier from its maximum extent marked by this moraine system resulted in large-scale glaciotectonic deformation of the glaciomarine sediments and the construction of a series of moraines, which are now largely buried by younger sediments but exposed in the coastal cliffs of Belgsholt and Melabakkar-Ásbakkar (see Fig. 1b) due to isostatic uplift following the final deglaciation (Sigfúsdóttir et al., 2018). The moraines record the periodic grounding of the retreating ice-margin and are composed of folded and thrusted glaciomarine sediments interleaved with penecontemporaneous ice-marginal sands and gravels (Sigfúsdóttir et al., 2018). The age of the deformed sediments range between c. 13.4 – 14.6 cal. ka BP (Ingólfsson, 1987, 1988; Norðdahl and Ingólfsson, 2015) indicating that the readvance probably occurred during the Younger Dryas or possibly later (Sigfúsdóttir et al., 2018). The age of the moraines become progressively younger northwards consistent with their formation at an oscillating ice margin during a phase of overall northward retreat (Sigfúsdóttir et al., 2018). The sedimentary basins formed between the moraines are infilled by well-bedded glaciomarine sediments, with the entire glacigenic sequence being unconformably overlain by littoral sands and gravels of early Holocene age (Ingólfsson, 1987, 1988).

METHODS

The large-scale glaciotectonics and stratigraphy of the Melabakkar-Ásbakkar cliff section have previously been described by Sigfúsdóttir et al., (2018) who divided this variably deformed glaciomarine sequence into eight informal sedimentary units (A-H); the same tectonostratigraphic framework has been adopted here. The detailed analysis of the macro- and microscale deformation structures associated with the emplacement of the thrust-bound blocks of glaciomarine sediments into the moraines is focused on the Melaleiti and Ásgil sections (Fig. 1b-d). Particular emphasis is placed upon understanding the nature of the deformation associated with the prominent thrust planes, which form the basal detachments to the allocthonous blocks.

A total of 16 orientated samples (Ásgil 1 to 10 from Ásgil and Mel 11 to 16 from Melaleiti) were collected from within these basal detachments for detailed micromorphological and microstructural analysis. Each sample was collected using a 10 x 10 x 5 cm aluminium Kubiena tin, which was carefully pushed or cut into the cliff face in order to limit sample disturbance. The position of the sample within the thrust zone, its orientation relative to magnetic north, depth and way-up were marked on the outside of the tin during collection. The samples were taken from different parts of the basal detachment in order to provide detailed information on the style and intensity of deformation within these glaciotectonic contacts, as well as examine the role played by pressurised water during the transport and emplacement of the thrust-blocks. Each sample was then removed from the face, sealed in two plastic bags to prevent drying out during transportation and cold storage prior to sample preparation at the British Geological Survey's thin section laboratory (Keyworth, Nottingham, UK). Sample preparation involves the replacement of pore-water by acetone, which is then progressively replaced by a resin and allowed to cure. Large format orientated thin sections were taken from the centre of each of the prepared samples, thus avoiding artefacts associated with sample collection. Each large format thin section was cut orthogonal to the stratification/bedding within the sediment and parallel to the main ice movement direction in the study area. The thin sections were examined using a standard petrological microscope and stereomicroscope allowing the detailed study of the microstructures at a range of magnifications. The terminology used to describe the various microtextures developed within these sediments in general follows that proposed by van der Meer (1987, 1993) and Menzies (2000) with modifications. Detailed maps of the range of sediments and microstructures present within the thin sections were obtained using the methodology of Phillips et al., (2010) (also see Neudorf et al., 2013; Vaughan-Hirsch et al., 2013; Phillips et al., 2013a). Due to the large number of thin sections analysed, microstructural analysis of the 12 most representative thin sections, which illustrate the complete range of structural relationships, are included in this paper. However, interpretive diagrams and high-resolution scans of the remaining four thin sections can be found as supplementary material.

RESULTS

The Ásgil thrust-block moraine

The ice-marginal thrust-block moraine at Ásgil comprises at least two stacked, gently northward dipping thrust-bound blocks of compact, weakly stratified to massive glaciomarine silt and sand (unit D; Fig. 2a; Sigfúsdóttir et al., 2018). The silt is poorly sorted, locally clay-rich, massive to weakly laminated and relatively thickly bedded (the thickest beds are over 1 m thick). The interbedded sand is sorted and considerably thinner bedded (up to~10 cm). The silt and sand largely retain their primary bedding but locally, mainly within the lower thrust-block, the sediments have undergone ductile shearing (augen structures and folds) and homogenisation. Each thrust-block is over 150 m long and about 10 m thick, and is dissected by a number of steeply inclined joints and southerly dipping normal (extensional) faults. Although not common, a small number of normal faults were observed cross-cutting the detachment separating the thrust-blocks, indicating that this phase of faulting post-dated the development of the thrust-stack. The base of the thrust-stack rests upon a few metre thick unit of stratified sand and gravel (unit B; Fig. 2a). These sands and gravels are folded and faulted, and record southward sense of shearing (based on vergence of folds and displacement along faults). The relative intensity of this deformation decreases towards the south. The sand and gravel can be traced laterally to the south of the thrust stack were they are unconformably overlain by a sequence of coarse gravel and boulders. This coarse-grained clastic sequence forms an over 15 m thick and 200 m wide multi-crested sediment pile located on the ice-distal side of the thrust stack. Based on its sedimentology and stratigraphic location, Sigfúsdóttir et al., (2018) interpreted this sequence as an ice-contact fan deposited during the same readvance which resulted in the construction of the adjacent thrust stack. Despite some localised folding and faulting this fan does not exhibit any macroscale glaciotectonic structures indicative of subglacial shearing, which suggests that the fan was not overridden after its formation.

The thrust-block moraine and the ice-contact fan rest on a glaciomarine diamicton (unit A of Sigfúsdóttir et al., 2018), which is exposed in the foreshore at low-tide. This silty-sandy diamicton probably directly overlies the underlying basalt bedrock as the latter crops out ~150 m further towards the northwest. The thrust-block moraine is overlain by an undeformed, glaciomarine sequence of interbedded silts, sands and diamictons (unit G; Fig. 2a) which were deposited after the glacier had retreated from this recessional limit. The glaciomarine sequence is in turn unconformably overlain by early Holocene littoral sand and gravel (unit H; Fig. 2a) deposited during the isostatic adjustment of the area (Ingólfsson, 1987, 1988).

At Ásgil the present study has focused on the deformation associated with the transport and emplacement along the basal detachment of the thrust-block moraine (see below).

Macroscale description of the basal detachment

Southeast of ~2550 m (Fig. 2a) the lowermost part (~0.5-1 m) of the thrust-block is characterised by a distinct zone of massive to laminated silt and sand, forming subhorizontal, locally cross-cutting sill-like features (Figs. 2b-c). The number of these layers increases downwards, towards the base of the thrust-block, indicating that their origin is related to the basal detachment of this thrust-block. Therefore this basal zone is inconsistent with representing a primary (sedimentary) bedded sequence. Consequently, the most likely origin of this complex zone is as a series of cross-cutting sediment-filled hydrofractures, which formed as pressurised water exploited the basal detachment of the developing thrust-block moraine (see below) (Rijsdijk et al., 1999; van der Meer et al., 1999; Phillips and Merritt, 2008; van der Meer et al., 2009; Phillips et al., 2013a; Ravier et al., 2015). Their cross-cutting relationships show that the grain size of the sediments infilling the hydrofractures increased with time. The largest sills (hydrofractures) are up to ~30 cm thick, have erosive margins and are infilled with coarse sand and granule-sized gravel. The sediments filling these hydrofractures also locally contain angular, elongate to tabular-shaped blocks (up to ~50 cm long, 10 cm thick) of fine-grained silt and sand which are lithologically similar to the marine sediments contained within the overlying thrust-block (Fig. 2c).

Although most of the hydrofractures form subhorizontal sill-like features, a number of high-angle to steeply inclined dykes dipping towards the southwest were also observed (Fig. 2c). These steeply inclined sediment-filled fractures are up to ~20 cm wide and ~8 m in length, and are filled by either a sandy-breccia or well-sorted, stratified sand and gravel; the latter often exhibit layering at an angle to the hydrofracture margins. These dyke-like features are rooted in the deformed basal zone and locally transect the entire thrust-block. They are often (but not always) wedge-shaped in form with the broadest part at the base of the thrust-block, tapering towards the top located higher in the cliff, possibly suggesting that these sediment-filled features propagated upwards from the base of the developing thrust-stack.

The relative intensity of deformation within the basal detachment of this imbricate thrust-stack gradually increases towards the north. Below this relatively thin deformed zone, in the southern part of the section, there is little evidence of glaciotectonic disturbance within the unit B sand and gravel indicating that negligible shear propagated downwards into these underlying deposits (Fig. 2b-c). In the northern part of the Ásgil section (between ~ 2450 and 2550; Fig. 2a) the contact between the thrust-block and the underlying unit B stratified sand and gravel is poorly defined. In this area, these two tectono-sedimentary units appear to have been partially intermixed, possibly due to liquefaction and injection of sand and gravel upwards into the base of the thrust-block resulting in large-scale brecciation and disruption within the overlying thrust-block (cf. Rijsdijk et al., 1999) (Fig. 2d). In the northern part of the section, the hydrofractures and their host deposits of unit D, as well as the underlying unit B sand and gravel are folded and thrust repeated, with the vergence of the folds recording a sense of shearing towards the south. Both sediment units and the boundary between them are cross-cut by minor faults, which cut the sediments at different angles.

Microscale deformation structures

Ten thin sections that were collected within the lowermost part of the thrust-block at Ásgil at three locations (Figs. 3, 4 and 5, see relative location on Fig. 2) in order to examine the deformation structures developed close to the southern leading edge of the thrust-block (at~2580-2590 m; Fig. 2a samples Ásgil 1-5; Fig. 3) and further north at a deeper structural level along the basal detachment (at 2520-2535 m; Fig. 2a samples Ásgil 6-10; Figs. 4 and 5). In thin section, the fine sand, silt and sandy diamicton, which not only form the thrust-block, but also the host sediments within the deformed, basal zone of the thrust-stack, are lithologically similar indicating that they were derived from a similar source (provenance).

Microstructures developed close to the leading-edge of the basal detachment (samples Ásgil 1-5)

The position of samples Ásgil 1-5 within the deformed zone marking the basal detachment close to the leading edge of the thrust-block moraine is shown in Fig. 3. These thin sections reveal that, although on a macroscale this zone appears highly deformed, this deformation is less apparent on a microscale with the samples being largely composed of finely stratified silt and silty-clay, with subordinate amounts of fine-sand (Figs. 6a-c). The contacts between these layers are undulating to irregular in form, and range from sharp to diffuse/gradational. The clay layers commonly possess a moderate to well-developed, layer-parallel plasmic fabric defined by optically aligned clay minerals. In sample Ásgil 4 (Fig. 6a) this birefringent clay (crossed polarised light) is locally fragmented with the fractures filled by homogenised silt and fine-sand. In sample Ásgil 2 (Fig. 6b) and, to a lesser extent, samples Ásgil 3 (Fig. 6c) and 4 (Fig. 6b), the stratification is offset by at least one set of gently to moderately northwest-dipping (apparent dip in plane of section provided by the thin sections) normal microfaults and a set of moderately southeast-dipping structures. These small-scale faults (displacements in the order of a few millimetres) appear to show a close spatial relationship to the lenses and layers of coarser grained sand.

The stratification within the fine silts and silty/sandy-clays is locally cross-cut and disrupted by irregular (erosive) lenses/layers of fine- to coarse-grained sand. These cross-cutting relationships indicate that the introduction of these coarser grained sediments post-dated the formation of the stratification within the finer grained sediments. The coarse-sand is matrix-poor (low clay content) and varies from massive (homogeneous) to weakly normal-graded (fining upwards). The coarse-sand grains are typically sub-rounded to rounded in shape, with the finer sand grains being more angular in appearance; possibly reflecting differences in the length of transport. Sand and gravel sized particles within these sediments are mainly composed of basaltic rock (lithic) fragments consistent with the predominantly basaltic bedrock in the region. Fresh, angular fragments of basaltic and silicic volcanic glass are also common detrital components. Detrital minerals present include plagioclase, pyroxene, olivine and opaque minerals, as well as minor zeolites and chlorite. In sample Ásgil 3, the introduction of the coarse-sand (see lower part of the thin section; Fig. 6c) resulted in the disruption/fragmentation of the adjacent stratified silt and fine-sand. This coarse-sand contains angular to irregular fragments of laminated silt and clay which are lithologically similar to, and therefore thought to have been derived from, the adjacent stratified sediments. Some of these clasts are composed of highly birefringent (under crossed polarised light) clay in which the optically aligned clay minerals define a moderate- to well-developed plasmic fabric. In samples Ásgil 2 (Fig. 6b) and 4 (Fig. 6a) the clay-clasts within the medium-sand layers are much smaller in size and are more rounded in shape, indicative of a greater degree of rounding (abrasion) during transport. In sample Ásgil 4 (Fig. 6a) the medium-sand layer near the bottom of the thin section is linked to a fine-scale network of fractures (veins) filled by the same sediment. This network is injected into the adjacent clay and comprises two subvertical sand-filled veins connected to a number of subhorizontal veins which occur parallel to the fine-scale lamination/stratification within the clay. The fine- to medium-sand layer in the upper part of this sample (Fig. 6a) contains a thin clay layer which is broken into a series of tabular segments with the intervening fractures filled by sand. Both the sand and clay layers are cross-cut by an irregular vein of pale coloured, medium-grained, matrix-poor sand. In the lower part of sample Ásgil 2 (Fig. 6b) the boundary between the medium- and fine-grained sand layers is complex and folded by a number of flame-like, asymmetrical disharmonic folds. The shape of these folds is consistent with an apparent sense of shear towards the southeast.

The microtextural relationships described above suggest that the sand layers were injected into the pre-existing stratified silts and clays. This process would have accompanied the brecciation and disruption of these fine-grained host sediments with the fragments dislodged from the walls of the developing sediment-filled hydrofracture being incorporated into the coarse-sand during the injection process. The cross-cutting relationships observed between the sand layers suggest that there were several phases of injection. The locally complex, irregular to folded boundaries to the sand layers observed in sample Ásgil 2 (Fig. 6b) suggests that the time interval between each phase of injection may have been relatively short. Injection of the later coarser grained sands, prior to the dewatering of the earlier formed sand, may have resulted in the observed soft-sediment deformation (disharmonic folding) in response to shear along the boundary between the two layers. In contrast, the more coherent silts and clays underwent brittle deformation with the normal (extensional) faulting as these stratified host sediments accommodated the expansion (increase in volume) of the sequence occurring in response to the injection of the liquefied coarse-sand. In samples Ásgil 2 (Fig. 6b), Ásgil 3 (Fig. 6c) and Ásgil 4 (Fig. 6a) the coarser sand layers occur parallel/sub-parallel to the stratification within the host silt and silty clay indicating that injection of these sediments exploited this pre-existing layering.

Samples Ásgil 1 (Fig. 6d) and Ásgil 5 (Fig. 6e) were taken from larger hydrofractures filled by a mud clast-rich breccia which is composed of elongated to irregular clasts of weakly stratified fine-sand, silt and clay set within a matrix of medium- to coarse-grained sand. The sandy matrix to the breccia varies from massive (sample Ásgil 1; Fig. 6d) to "patchy"/"mottled" in appearance due to the variation in its grain-size from fine- to coarse-sand (sample Ásgil 5; Fig. 6e). Sample Ásgil 1 was taken from the margin of a prominent (up to 20 cm wide, 8 m long), steeply southeast dipping sediment-filled fracture system that cross-cuts fine-grained weakly layered clayey-silt, silt and fine sand at the base of the thrust-block (Figs. 3a, c). Whereas, sample Ásgil 5 (Fig. 6e) was collected from a c. 50 cm wide, subhorizontal breccia-filled hydrofracture that cuts through the finely layered sediments at the base of the thrust-block (Figs. 3a, b). The laminated silt and clay clasts within the breccia range from angular to rounded in shape; possibly reflecting a variation in the degree of rounding (abrasion) of the clasts during transport and injection of this coarse-grained sediment into the developing hydrofracture. However, the degree of rounding of these clasts appears to be dependent upon lithology, with the sandy intraclasts tending to be more rounded in shape with more diffused clast margins. The orientation of bedding preserved within the large clasts indicate that during transport (injection) they have been rotated (tilted) and possibly overturned. The clay layers within the clasts are locally broken and the fractures infilled by silt and fine-sand, indicating that these sediments have potentially recorded several phases of liquefaction, remobilisation and injection prior to brecciation associated with the formation of the large-scale hydrofracture system. In sample Ásgil 1 (Fig. 6d) the margins of the hydrofracture are irregular and it appears that some of the clasts contained within the breccia have been ripped (eroded) from the stratified sediments forming the "wall-rock" to this fracture system. Elongate clasts immediately adjacent to the wall of the hydrofracture show a preferred shape-alignment parallel or, at a low-angle to the margin of the fracture (Fig. 6d). In contrast, towards the interior of the vein the clasts are apparently more randomly orientated or may possibly define a subhorizontal preferred shape-alignment (see Fig. 6d). In the lower, southeast corner of the thin section the breccia is cut by a complex network of clay veins. These veins are filled by finely laminated, highly birefringent clay (cutan). The sediments forming the host to this breccia-filled hydrofracture occur on the left-hand (northern) side of the thin section (Fig. 6d). The weakly developed to diffuse stratification developed within these silts and fine-sands has an apparent dip towards the southeast. In the lower right-hand corner of the thin section this stratification is cross-cut by two thin (< 10 mm) sediment-filled veins composed of clay and sandy-clay (Fig. 6d). The larger of these two veins is layered with an outer layer of clay lining the fracture walls and a central infilling of massive clayey-sand. A similar clay-filled, southwest-dipping vein was also observed cutting through the breccia within sample Ásgil 5 (Fig. 6e) were it is filled by weakly layered clayey-silt and silt with this layering occurring parallel to the fracture walls.

Microstructures developed at a deeper structural level of the basal detachment (samples 6-10)

Thin sections Ásgil 6-10 (Figs. 7-8, S1) were collected within the deformed zone associated with the basal detachment at a deeper structural level at the thrust-block moraine (Figs. 4 and 5). Sample Ásgil 9 (Supplementary Figure 1) was collected from the thrust-block and comprises homogenised silts and sands (a diamicton). Samples Ásgil 8 and 10 (Fig. 7) were taken from fine-grained sediments comprising the base of the thrust-block and samples. Ásgil 6 and 7 (Fig. 8) were taken from subhorizontal hydrofractures that cross-cut these fine-grained deposits (Fig. 4 and 5).

Thin sections Ásgil 8 and Ásgil 10 (Fig. 7) are dominated by finely stratified silty-clay, silt and very fine-sand which are lithologically similar (grain size, sorting and stratification) to the finely stratified clay, silt and sand forming the host to the hydrofracture system in samples Ásgil 1-5 (Fig. 6). However, much more disruption is observed in samples Ásgil 8 and 10 (Fig. 7). The sediments have a mottled appearance as the stratification is diffused/gradational and the beds/laminae are undulating and discontinuous. This may possibly be due to an increase in the amount of layer-parallel shear accommodated by the laminated sediments within this structurally deeper and more complex part of the basal detachment. In sample Ásgil 8 (Fig. 7a) the stratification is mostly subhorizontal/weakly folded with the disruption of the layers increases upwards. The stratification is offset by a poorly defined, conjugate set of normal microfaults with apparent dips both towards the NW and SE. In the lower part of this finely stratified subunit the faults have a moderate to steep dip, but in the upper part the faults tend to have lower dips. In the upper part of sample Ásgil 8 (Fig. 7a) the layers are tilted between two of these low-angle faults resulting in an asymmetrical S-shaped layering between these two faults. The faulted and folded stratified sediments are truncated by an apparently SE dipping sand-vein (see Fig. 7a). The vein is about 0.5 cm thick with sharp boundary and a step-like form, and is infilled with massive fine-grained sand with high intergranular porosity. The geometry and the erosive nature of the infilling is consistent with this sand-vein being a hydrofracture. A larger sand-vein/hydrofracture dominates the lowermost part of thin section Ásgil 8 (Fig. 7a). This hydrofracture is seen in the lower~4 cm of the thin section where it has an apparent dip towards the northwest. The sediments within it comprise medium-grained sand that is lithologically similar to the sands seen in samples Ásgil 6 and Ásgil 7 (see below). The sand typically possesses a high intergranular porosity and low matrix content. The individual sand grains are subrounded to angular in shape. Within the sand are fragmented silt and clay laminae, as well as variably aligned fragments (intraclasts) of silty-clay which define a weakly developed/preserved layering which dips towards the northwest. The intraclasts have smooth edges indicative of rounding during transport. The upper boundary of the hydrofracture is defined by~1 cm thick deformed layer of unsorted silt, sand and clay that is offset by a set of northwest-dipping faults associated with small-scale folds. The faults are cross-cut by the sand-vein so the injection of the sand post-dated the small-scale faulting of the host sediments. In sample Ásgil 10 (Fig. 7b), the stratification within the clayey-silt/silty-clay is highly disrupted and the laminae are tilted, folded and possibly overturned. In between the clay-rich layers which dominate the thin section are layers of sorted silt and very fine sand with sharp boundaries. In the middle-upper part of the thin section is a lens of coarse-grained sand with diffused edges. All these sediments are dissected by a number of faults. The faults are poorly defined and some have sand-lining possibly deposited by water flowing along the fault walls. The faults have a very gentle to moderate dip towards the southeast (apparent dip) but due to complex deformation of the sample it was difficult to estimate the direction of offset along the fault planes although most of them appear to record apparent displacement towards the southeast.

Samples Ásgil 6 and 7 (Fig. 8) were taken from subhorizontal layers of sand with erosional margins, consistent with being hydrofractures (Fig. 4). The thin sections show that the sand within the hydrofractures is weakly stratified- to heterogeneous, and is interbedded with layers of silt and clayey-silt possibly reflecting fluctuations of the velocity of the water flowing through the fractures. The sand is fine- to medium-grained and possesses an intergranular porosity and variable amounts of a fine-grained matrix. Most of the sand grains are subrounded to angular in shape and composed of a similar range of components to the sand layers in samples Ásgil 1-5 (Fig. 6). The contacts between the layers are irregular and the silty-clay layers tend to be very fragmented, possibly due to brecciation of the rigid clay layers in response to the liquefaction and ductile deformation of the open-packed silt and sand. Although the alignment of elongate clasts appears to preserve the original stratification within the hydrofractures some of the clay fragments are randomly dispersed within the sand indicating longer transport path of these clasts. These "dispersed" fragments tend to have rounded and rather diffuse edges. The weakly preserved stratification is deformed by a number of upright to steeply inclined, asymmetrical, southeast-verging folds (Fig. 8). This indicates that after the hydrofractures formed, the sediments underwent a minor ductile shearing, possibly as a result of transmission of shear into the deposits during the thrust-block transport.

Overall samples Ásgil 6 to 8 and 10 (Figs. 7-8) show higher intensity of faulting and folding compared to thin sections Ásgil 1-5 (Fig. 6). This is consistent with the observed, larger-scale increase in complexity and magnitude of deformation towards the northern, structurally deeper part of the detachment. The lithological similarities and the tectonostratigraphic location of the finely layered silty-clay, silt and sand (see Ásgil 8 and 10, Fig. 7) to those seen at the front of the thrust (Ásgil 1 to 5. Fig. 6) may suggest that these are part of the same deformation zone. However, they have lost some of their identity due to folding and faulting resulting from increased shearing transmitted into the deposits, probably during the thrust stacking. This phase of shearing was followed by a renewed phase of sediment liquefaction and injection resulting in sediment brecciation and hydrofracturing. The hydrofractures developed both parallel to bedding and to earlier formed thrusts and faults. The final deformation phase involved folding and faulting of both the hydrofractures and their host deposits (Ásgil 6 to 8 and 10, Figs. 7-8) indicating increased draining of the deforming sequence.

Melaleiti thrust-block moraine

The thrust-block moraine at Melaleiti is over 300 m across and 10 m high, and comprises several, subhorizontal or gently north-dipping, stacked thrust-bound allochthonous blocks (Fig. 9). Each block is composed of two main sedimentary units; a massive, silty-sandy, very compact and deformed glaciomarine diamicton of unit A, and unit E consisting of interbedded silt and sand of with occasional, thin layers of gravel and diamicton (Sigfúsdóttir et al., 2018). The thrust-blocks are dissected by a large number of normal (extensional) faults with a dominant dip towards the southeast (Fig. 9), although some dip towards the northwest. The relative complexity of deformation decreases to the southwest (ice-distal part) as can be seen in a decrease in the intensity of faulting/thrusting and better preservation of primary sedimentary in sediment units E. This probably reflects a decrease in strain away from the ice-front during the thrust-stacking (Sigfúsdóttir et al., 2018).

The moraine is overlain by an up to 2 m thick unit of coarse gravel (unit F on Fig. 9a). This unit is interpreted as having been deposited under high pressure in subglacial setting, which indicates that the moraine was overridden by the glacier.However it is unclear if it was overridden by the same or a younger advance (Sigfúsdóttir et al., 2018). The original structure of the moraine is preserved indicating that it did not undergo extensive subglacial deformation during the overriding. However, some of the normal faults that cross-cut (postdate) the thrusts-bound blocks were possibly developed in response to extensional deformation as the glacier overrode the moraine (Sigfúsdóttir et al., 2018).

Macroscale description of the basal detachment

This study focuses on an over 150 m long detachment in the southernmost part of the thrust stack (~100-250 m; Fig. 9a). The base of the thrust-block is very sharp and the deposits in the footwall (both unit E and A) are variably deformed. The relative intensity of this deformation decreases southwards towards the leading edge of the thrust-block moraine. In the northern part, between ~100 and 180 m, the sediments are deformed by numerous folds and boudins which are cross-cut by normal and reverse faults as well as subhorizontal shears (Fig. 9b). The geometry of these structures suggests that they developed as Reidel shears within the footwall of the detachment at the base of the thrust-block (Phillips and Lee, 2011). The majority of the normal and reverse faults do not cross-cut the main detachment, indicating that they predated or were developed at the same time as this larger scale structure. Closer to the leading edge of the thrust-block moraine (between~180 and 300 m; Fig. 9a) the bedded silts and sands have undergone less penetrative deformation. For example, the bedded unit E sediments are relatively intact although cross-cut by a large number of well-defined, southeast and northwest-dipping normal faults (Fig. 9c). Based upon the observed cross-cutting relationships these faults are interpreted as both pre-dating and post-dating the thrust-detachment. A small number of the faults are infilled/lined by massive and stratified sand indicating that these fractures acted as fluid pathways. These hydrofractures are relatively thin (up to ~3 cm) and usually they cross-cut other structures indicating that they were formed during late-stage of the deformation (Fig. 9d).

Microscale deformation structures

Six thin sections were taken from samples collected at ~110 m (Fig. 9a), from the glaciomarine interbedded silt, sand and diamictons of unit E located immediately below the southernmost thrust-detachment (Fig. 10). Three of them are described below (Mel 11, 14 and 16; Fig. 11), the remaining three (Mel 12, 13, 15) are available as supplementary material (Supplementary Figure 2). The Mel 11 to 16 thin sections are composed of moderately to well sorted, open packed, fine to medium grained sand (Figs. 11, Supplementary Figure 2). The sand grains are usually subrounded to angular in shape and mainly consist of basaltic rock (lithic) fragments. Fresh, angular fragments of volcanic glass are also common, the content of the lighter coloured, silicic tephra being higher compared to the sand within the detachment at Ásgil. Other minerals include plagioclase, pyroxene, olivine and opaque minerals, as well as minor zeolites and chlorite. The sand layers are interbedded with thinner layers of silt and silty-clay. The contacts between well-sorted silt and sand layers are commonly diffusive and locally they appear interdigitate, which could indicate local liquefaction and subsequent mixing of these sediments. The more rigid, clay-rich layers have undergone brecciation and extension (boudinage), most likely in response to/accompanying the liquefaction of the adjacent sand (Fig. 11). Locally the clayey intraclasts are dispersed within the fluidised silt and sand (see upper part in sample Mel 16; Fig. 11a); although they usually have sharp edges and are often aligned and partly preserve the primary layering indicating short transport path. The bedded/laminated clays, silts and sands are locally folded with the vergence of folds recording an apparent sense of shear towards the southwest (see Mel 14; Fig. 11b). In the lower half of thin section Mel 11 (Fig. 11c) the folded, bedded/laminated clay, silt and sand are cross-cut by vein infilled by open-packed fine sand. Within this sand layer, there are intraclasts of laminated sand, silt and clay with smooth edges. This relationship suggests that the sand layer was injected into the pre-existing interlaminated sediment resulting in hydrofracturing and brecciation of the host sediments. Intraclasts from the host-sediments would then be incorporated into the sediments being injected into the developing hydrofracture. As described above, the deformed unit E sediments are cross-cut by number of shears and faults, some of which are clearly visible in thin section (e.g. Mel 16; Fig. 11a).

DEVELOPMENT OF THE ÁSGIL AND MELALEITI THRUST-BLOCK MORAINES: A SEQUENTIAL MODEL AND DISCUSSION

The detailed macro- and microscale study of the detachments within the Ásgil and Melaleiti thrust-moraines show that their development was accompanied by repeated phases of sediment liquefaction, injection and hydrofracturing. The observed microstructural relationships indicate that these processes occurred during the transport and emplacement of the autochthonous sediment blocks. This sequence of events associated with the detachment, transport and emplacement of thrust blocks in the moraines can be explained in terms of the detailed five-stage model (Fig. 12).

Stage 1: Detachment

The structural architecture of the moraines exposed in Melabakkar-Ásbakkar indicates that they formed in response to south/south-eastward directed ice-push by a glacier advancing from Borgarfjörður (Fig. 1b) (Ingólfsson, 1987, 1988; Sigfúsdóttir et al., 2018). Thus, the thrust-blocks comprising the moraines at Ásgil and Melaleiti can be assumed to be derived offshore, north/north-west of the study site (Fig. 1). As the moraines were formed in a submarine setting (Ingólfsson 1987, 1988; Sigfúsdóttir, 2018), the sediment blocks that were detached, displaced and stacked to form the thrust-block moraines were presumably unfrozen and water-saturated during glaciotectonism.

The earliest phase of deformation recorded by the thrust-block sediments at Ásgil is the liquefaction of the silt and fine-grained sand layers towards the base of the thrust-block, indicative of increasing porewater pressures within the sediments as they are being deformed. The liquefaction of the sediment would have dramatically lowered its shear strength facilitating deformation and enabling low-frictional detachments to form within the substratum (Moran et al., 1980; Bluemle and Clayton, 1984; Phillips et al., 2007; Phillips and Merritt, 2008; Burke et al., 2009; Vaughan-Hirsch et al., 2013) (Fig. 12, stage 1). The detachments typically develop within weak, sand and silt layers contained (sealed) between more impermeable layers (clay, bedrock) enabling porewater pressures to build up within these coarser grained sediments (Bluemle and Clayton, 1984; van der Wateren, 1985; Croot, 1987; Boulton and Caban, 1995; Phillips and Merritt, 2008; Vaughan-Hirsch and Phillips, 2017) (Fig. 12, stage 1). Consequently laterally extensive, subhorizontal beds of sand within the glaciomarine deposits at Melasveit are considered to have provided a focus for initial deformation, leading to thrust propagation and the detachment of the slab-like sediment-blocks.

Elevated porewater-pressures within ice-marginal/proglacial sediments are likely to occur due to ice load, tectonic thickening as well as basal shear stress applied by the advancing glacier (van der Wateren, 1985; Boulton and Caban, 1995). Also, it is likely that preferential flow of subglacial meltwater towards the ice margin from compressed subglacial deposits further up-glacier and/or external sources (i.e surface melting) might have contributed to further elevate the water content/pressures within the deforming sequence (Boulton et al., 2001, Vaughan-Hirsch and Phillips, 2017). Syntectonic subaquatic outwash sediments forming lenticular aprons/fans along the leading edge of some of the moraines in Melasveit (i.e. Ásgil) indicate that the large-scale glaciotectonism at Melasveit was associated with high meltwater fluxes (Sigfúsdóttir et al., 2018). This relationship may be used to suggest that the advances that resulted in formation of the moraines were a result of accelerated ice-flow or possibly surging (e.g. Kamb et al., 1985; Piotrowski and Tulaczyk, 1999; Fischer and Clarke, 2001; Kjær et al., 2006; Phillips et al., 2013; Phillips et al., 2018).

Stage 2: Pro-glacial/ice-marginal thrusting and movement along the décollements

Due to gravity spreading caused by the weight gradient at the ice margins and compression from the rear caused by ice flow (Fig. 12, stage 2) (Rotnicki, 1976; van der Wateren, 1995; Pedersen, 1987; Aber et al., 1989; van der Wateren, 1995; Bennett, 2001; Pedersen, 2005; Aber and Ber, 2007; Sigfúsdóttir et al., 2018), the detached sediment blocks would have been “pushed”/”displaced” forward by the advancing glacier (Fig. 12, stage 2). The transport of the allochthonous sediment blocks was most likely aided by continued elevated porewater pressures and fluid flow being maintained along the earlier formed detachments. Evidence for this is provided by the repeated phases of liquefaction and injection along these décollement surfaces; thereby minimising the amount of shear being transmitted into the adjacent sediments and facilitating the displacement of the large slabs of unconsolidated sediments by the advancing ice. The detachments would have acted as fluid pathways, focusing water escape within the relatively clay-rich glaciomarine sequence and facilitating the southward migration of water through the deforming sediment pile.

At Ásgil, the complex, cross-cutting sets of hydrofractures and associated brecciation of the sediments within the base of the thrust-block clearly indicate that water pressures within the deforming sediment pile repeatedly exceeded the cohesive strength of these deposits. Field and thin section evidence clearly indicates that the grain size of the sediments infilling this evolving hydrofracture system increased over time, accompanied by an increase in the size (width/length) of the individual sediment-filled fractures (Fig. 12, stage 2). Well-defined, sharp, erosive contacts between the hydrofractures show that they were probably formed in response to several phases of injection and fragmentation of the sediments between periods of partial solidification of the deposits rather than gradual changes in flow regime during a single event (Fig. 12, stage 2). These variations could either be due to fluctuations in the submarginal hydrology (water input) or release of hydrostatic pressure due to periodic water escape towards the front of the evolving imbricate thrust stack potentially resulting in a stick-slip type of movement along the thrusts (Boulton et al., 2001; Phillips and Merritt, 2008).

Stage 3: Development of the thrust-block moraines

The dislocated thrust-blocks were accreted at the ice-margin leading to the formation of the glaciotectonic thrust-block moraines (Fig. 12, stage 3). At Melaleiti the thrust-blocks were emplaced upon less compact and permeable sequence of interbedded silt, sand and gravel of the underlying thrust blocks. Similarly, at Ásgil, the detached thrust-blocks were emplaced upon a sequence of ice-marginal sands and gravels, which were deposited at an earlier stage during the readvance. Despite the high-permeability of these underlying deposits, which would have facilitated draining of the proposed water-lubricated basal detachments to the thrust-blocks, the lowermost block is thought to have been transported across the coarser grained sediments in the footwall resulting in little disturbance of these deposits below the leading edges of the thrusts (Fig. 12, stage 2). This is thought to indicate that initially, the thrust-blocks where in effectively "decoupled" from the underlying sediments, possibly indicating that the rate of subglacial meltwater being transmitted through the basal detachment temporarily exceeded the rate at which water was dissipated through the footwall sediments. The subaquatic setting might have aided this process as the footwall sediments will have been water saturated.

Eventually, however, the presence/introduction of highly permeable sand and gravel within the footwall of the thrust is thought to have resulted in the dewatering of this basal detachment. The reduction of the porewater content/pressure within this detachment will have led to an increase in the cohesive strength of the sediments within this zone leading to an increase in friction drag between the allochthonous thrust-block (hanging-wall) and the underlying footwall sediments. This process would have resulted in the locking-up of the basal décollement and accretion of the thrust-block onto the up-ice side of the evolving glaciotectonic landform (Fig. 12, stage 3).

The northwards increase in the relative intensity of deformation (folding, faulting) within the up-ice sections of both the Ásgil and Melaleiti moraines is consistent with an increase in the amount of shearing within the structurally deeper parts of the evolving glaciotectonic landforms (Fig. 12, stage 3). Detailed analysis of the thin sections taken from both from the base of the thrust-blocks and the footwall sediments within the structurally deeper parts of the moraines reveal that this deformation involved a complex interplay between ductile shearing (folding and faulting) and sediment liquefaction, injection, hydrofracturing and brecciation (Fig. 12, stage 3).

Large hydrofractures formed within the Ásgil moraine during this phase, especially within the inner part of the moraine, extend from the sands and gravels in the footwall, cutting upwards into the overlying thrust-block. This field evidence suggests that this phase of hydrofracturing and water escape post-dated the emplacement of the structurally lower thrust-block within the moraine. This may be used to suggest that the pressures within the subglacial hydrogeological system were increasing during glacitectonism, possibly due to increasing overburden pressures during the displacement and accretion of the thrust-blocks onto the up-ice side of the evolving glaciotectonic moriane. Alternatively, the impermeable sediment within the large thrust-blocks, coupled with the deposition of an ice-marginal fan/apron, may have also impeded the escape of meltwater water from beneath the ice margin, resulting in an increased hydrostatic pressure within the subglacial hydrogeological system.

Stage 4: Emplacement

The combination of a fall in water pressures within the deforming sediments coupled with fluid escape towards the leading edge of the evolving thrust stack would have resulted in dewatering of deforming sediment pile (Fig. 12, stage 4). This would have led to continued increased friction between the base of the thrust-blocks and underlying deposits (Phillips et al., 2007; Benediktsson et al., 2008, 2010) leading to the progressive cessation of displacement of the allochthonous blocks and their accretion onto the up-ice side of the evolving thrust-block moraine. At both Ásgil and Melaleiti the earlier formed ductile deformation structures (folds and shears) are post-dated by later faulting and thrusting, recording a switch from ductile to brittle deformation associated with the dewatering of the deforming sequence. The cross-cutting relationship between the faults and the detachments at the base of the thrust-blocks clearly indicate that these moderate to high-angle brittle structures developed both prior to, and after the final emplacement of the thrust-blocks. At Ásgil, most of the faults are small and only record minor displacement (up to few dm). However at Melaleiti, larger scale faults and subhorizontal shears were observed cross-cutting the earlier developed ductile structures developed within the high-strain zone marking the base of the thrust-blocks. Most of the faults dip towards the southeast (down-ice) consistent with these faults having formed as down-ice dipping Reidel shears in response to simple shear (c.f. Phillips and Lee, 2011), possibly imposed by the overriding, structurally higher thrust-block as it “slid over” the underlying thrust-block which was already emplaced into the moraine.

Stage 5: *Overriding*

Field evidence suggests that the glacier overrode the Melaleiti moraine, accompanied by the deposition of the coarse-grained meltwater deposits at the base of the overlying ice mass (Fig. 12; stage 5) (Sigfúsdóttir et al., 2018). The water eroded the uppermost part of the moraine. However, sedimentary features and structures formed by thrusting are well-preserved indicating that the moraine did not experience extensive subglacial deformation during the overriding. Possibly high water pressures at the base of the glacier minimised transmission of shear into the underlying deposits allowing the preservation of the underlying landforms.

Wider implications

Blocks of sediments that have been detached and transported by glaciers are widespread in past glaciated regions, both in the terrestrial and marine environment (Bluemle and Clayton, 1984; Ruszczynska-Szenajch, 1987; Aber and Ber, 2007; Phillips and Merritt, 2008; Benn and Evans, 2010; Vaughan-Hirch et al., 2013; Rüther et al., 2013; Vaughan-Hirsch and Phillips, 2017). For example, they can occur as isolated sediment or bedrock megablocks or rafts scattered over large areas (Aber and Ber, 2007; Rüther et al., 2013; Vaughan-Hirsch et al., 2013; Benn and Evans, 2010) or, stacked with deformed sediments to form a range of glaciotectonic landforms comparable to the moraines observed at Melasveit (Croot, 1987; Huddart and Hambrey, 1996; Pedersen, 2005; Bennett, 2001; Benediktsson et al., 2008, 2010; Burke et al., 2009; Vaughan-Hirsch and Phillips, 2017; Phillips et al., 2017). The Melaleiti and Ásgil moraines can be both classified as thrust-block moraines (see Benn and Evans and references therein) and are characterised by are number of stacked, low-angle/subhorizontal thrust-blocks which show very little evidence of large-scale folding. The geometry of the moraines is typical for moraines formed by low-frictional sliding, supported by the relatively rigid nature of the thrust-block deposits (van der Wateren, 1995; Huddart and Hambrey, 1996; Boulton et al., 1999; Bennett, 2001). Although it has been shown that presence of pressurised water along décollements/thrust-planes is important for forward movement of sediment blocks/thrust-blocks both in subglacial and ice-marginal setting (Moran et al., 1980; van der Wateren, 1985; Broster and Seaman, 1991; Boulton and Caban 1995; Pedersen, 2005; Kjær et al., 2006; Benediktsson et al., 2008, 2015; Phillips and Merritt, 2008; Vaughan-Hirsch and Phillips, 2017; Phillips et al., 2017) Only few studies have dealt with the detailed, microscale events taking place along major detachments (Phillips and Merritt, 2008; Vaughan-Hirsch et al., 2013) hampering our understanding on the conditions governing the detachments and dislocation of such sediment blocks. The microscale structures investigated in this study record processes that occurred during detachment, transport and accretion of large sediment blocks found within thrust-block moraines. In summary it shows that the presence of over-pressurised porewater within detachments play key role in the transport. Furthermore, this study provides clear evidence for preservation of the unfrozen and unlithified sediment blocks during glaciotectonic thrusting.

CONCLUSIONS

In this paper we proposed a detailed structural model for processes occurring during glaciotectonic thrusting based on micro-scale study of detachments within two ice-marginal thrust-block moraines.

- The initial detachment of the sediment blocks most-likely took place in response of ice-push and gravity-spreading at the margins of the advancing glacier. Over-pressurizing of groundwater relating to the advance lead to fluidisation of sorted silts and sand layers within the bedded/laminated glaciomarine sediments and formation of detachments along these water lubricated layers.
- The transport of the sediment blocks was aided by continued elevated porewater pressures being maintained along the detachments resulting in repeated phases of sediment liquefaction. This minimised the amount of shear transmitted into the surroundings allowing the large unconsolidated and unfrozen sediment-blocks sediment blocks to be transported by the glacier.
- Water pressures within the deforming sediment pile repeatedly exceeded the cohesive strength of these sediments during emplacement and the accretion of the thrust block resulting in hydrofracturing and fluid escape. That was followed by periodic partial draining and transmission of shear most notably in the structurally deeper parts of the evolving moraines where overburden pressures where higher and drainage more restricted.
- The combination of a fall in water pressures within the deforming sediments coupled with fluid escape resulted in dewatering of the sediments. This leading to increased friction between the base of the thrust-blocks and underlying deposits causing increased brittle deformation (faulting) and lock-up of the thrust-blocks.
- The hydrogeology along with the lithological characteristics of the deforming sediments played key in controlling the changing style of deformation during the detachment, transport of the sediment-blocks and in the accretion of the moraines.

ACKNOWLEDGEMENTS

This project was funded by the Icelandic Research Fund (grant no. 141002-051 to Í. Ö. Benediktsson) and the Royal Physiographic Society in Lund (grants to T. Sigfúsdóttir and Í. Ö. Benediktsson). Additional support was provided by the British Geological Survey (to E. Phillips). We would like to thank Heimir Ingimarsson, Sandrine Roy and Kim Teilmann for their assistance in the field.

REFERENCES

Aber, J.S., 1988. Ice-shoved hills of Saskatchewan compared with Mississippi Delta mudlumps: implications for glaciotectonic models. In: Croot, D.G. (Ed.), Glaciotectonic Forms and Processes. Balkema, Rotterdam, pp. 1-9.

Aber, J.S., Ber, A., 2007. Glaciotectonism.. Development in Quaternary Science 6. Elsevier, Amsterdam.

Aber, J.S., Croot, D.G., Fenton, M.M., 1989. Glaciotectonic landforms and structures. Kluwer, Dordrecht.

Alley, R., 1989. Water-Pressure Coupling of Sliding and Bed Deformation: I. Water System. Journal of Glaciology 35, 108-118.

Andreassen, K., Ødegaard, C.M., Rafaelsen, B., 2007. Imprints of former ice streams, imaged and interpreted using industry three-dimensional seismic data from the south-western Barents Sea. Geological Society, London, Special Publications 277, 151-169.

Banham, P.H., 1975. Glaciotectonic structures: a general discussion with particular reference to the contorted drift of Norfolk. Seal House Press, Liverpool,

Baroni, C., Fasano, F., 2006. Micromorphological evidence of warm-based glacier deposition from the Ricker Hills Tillite (Victoria Land, Antarctica). Quaternary Science Reviews 25, 976-992.

Benediktsson, Í.Ö., Möller, P., Ingólfsson, Ó., van der Meer, J.J.M., Kjær, K.H., Krüger, J., 2008. Instantaneous end moraine and sediment wedge formation during the 1890 glacier surge of Brúarjökull, Iceland. Quaternary Science Reviews 27, 209-234.

Benediktsson, Í.Ö., Schomacker, A., Johnson, M.D., Geiger, A.J., Ingólfsson, Ó., Guðmundsdóttir, E.R., 2015. Architecture and structural evolution of an early Little Ice Age terminal moraine at the surge-type glacier Múlajökull, Iceland. Journal of Geophysical Research: Earth Surface 120, 1895-1910.

Benediktsson, Í.Ö., Schomacker, A., Lokrantz, H., Ingólfsson, Ó., 2010. The 1890 surge end moraine at Eyjabakkajökull, Iceland: a re-assessment of a classic glaciotectonic locality. Quaternary Science Reviews 29, 484-506.

Benn, D.I., Evans, D.J.A., 2010. Glaciers and Glaciation. Hodder Education, London.

Bennett, M.R., 2001. The morphology, structural evolution and significance of push moraines. Earth-Science Reviews 53, 197-236.

Bluemle, J.P., Clayton, L., 1984. Large-scale glacial thrusting and related processes in North Dakota. Boreas 13, 279-299.

Boulton, G.S., Caban, P., 1995. Groundwater flow beneath ice sheets: Part II — Its impact on glacier tectonic structures and moraine formation. Quaternary Science Reviews 14, 563-587.

Boulton, G.S., Dent, D.L., Morris, E.M., 1974. Subglacial Shearing and Crushing, and the Role of Water Pressures in Tills from South-East Iceland. Geografiska Annaler: Series A, Physical Geography 56, 135-145.

Boulton, G.S., Dobbie, K.E., Zatsepin, S., 2001. Sediment deformation beneath glaciers and its coupling to the subglacial hydraulic system. Quaternary International 86, 3-28.

Boulton, G.S., Van der Meer, J.J.M., Beets, D.J., Hart, J.K., Ruegg, G.H.J., 1999. The sedimentary and structural evolution of a recent push moraine complex, Holmstrombreen, Spitsbergen. Quaternary Science Reviews 18, 339-371.

Broster, B.E., Seaman, A.A., 1991. Glacigenic rafting of weathered granite. Canadian Journal of Earth Sciences 28, 649-654.

Burke, H., Phillips, E.R., Lee, J.R., Wilkinson, I.P., 2009. Imbricate thrust stack model for the formation of glaciotectonic rafts: an example from the Middle Pleistocene of north Norfolk, UK. Boreas 38, 620-637.

Clayton, L., Moran, S.R., 1974. in: Coates, D.R. (Ed.), Tills and Glaciotectonics. Balkema, Rotterdam, pp. 183-195.

Croot, D.G., 1987. Glacio-tectonic structures: a mesoscale model of thin-skinned thrust sheets? Journal of Structural Geology 9, 797-808.

Evans, D.J.A., 2018. Till- A glacial process sedimentology. Wiley-Blackwell.

Evans, D.J.A., England, J., 1991. High Arctic thrust block moraines. The Canadian Geographer / Le Géographe canadien 35, 93-97.

Fischer, U.H., Clarke, G.K.C., 2001. Review of subglacial hydro-mechanical coupling: Trapridge Glacier, Yukon Territory, Canada. Quaternary International 86, 29-43.

Franzson, H., 1978. Structure and petrochemistry of the Hafnarfjall-Skarðsheiði Central Volcano and the surrounding basalt succession, W-Iceland. The University of Edinburgh, p. 264.

Hiemstra, J., & Van Der Meer, J, 1997. Pore-water controlled grain fracturing as an indicator for subglacial shearing in tills. . Journal of Glaciology 43, 446-454.

Huddart, D., Hambrey, M. J., 1996. Sedimentary and tectonic development of a high-arctic, thrust-moraine complex: Comfortlessbreen, Svalbard. Boreas 25, 227-243.

Ingólfsson, Ó., 1987. The Late Weichselian glacial geology of the Melabakkar-Asbakkar coastal cliffs, Borgarfjörður, W-Iceland. Jökull 37, 57-81.

Ingólfsson, Ó., 1988. Glacial history of the lower Borgarfjördur area, western Iceland. Geologiska Föreningens i Stockholm Förhandlingar 110, 293-309.

Ingólfsson, Ó., Norddahl, H., 2001. High Relative Sea Level during the Bolling Interstadial in Western Iceland: A Reflection of Ice-sheet Collapse and Extremely Rapid Glacial Unloading. Arctic, Antarctic, and Alpine Research 33, 231-243.

Ingólfsson, Ó., Norddahl, H., Schomacker, A., 2010. 4 Deglaciation and Holocene Glacial History of Iceland, in: Schomacker, A., Krüger, J., Kjær, K.H. (Eds.), Developments in Quaternary Sciences. Elsevier, pp. 51-68.

Jennings, A., Syvitski, J., Gerson, L., Grönvold, K., Geirsdóttir, Á., Hardardóttir, J., Andrews, J., Hagen, S., 2000. Chronology and paleoenvironments during the late Weichselian deglaciation of the southwest Iceland shelf. Boreas 29, 163-183.

Kamb, B., Raymond, C.F., Harrison, W.D., Engelhardt, H., Echelmeyer, K.A., Humphrey, N., Brugman, M.M., Pfeffer, T., 1985. Glacier Surge Mechanism: 1982-1983 Surge of Variegated Glacier, Alaska. Science 227, 469-479.

Khatwa, A., Tulaczyk, S., 2001. Microstructural interpretations of modern and Pleistocene subglacially deformed sediments: the relative role of parent material and subglacial processes. Journal of Quaternary Science 16, 507-517.

Kjær, K.H., Larsen, E., van der Meer, J., Ingólfsson, Ó., Krüger, J., Örn Benediktsson, Í., Knudsen, C.G., Schomacker, A., 2006. Subglacial decoupling at the sediment/bedrock interface: a new mechanism for rapid flowing ice. Quaternary Science Reviews 25, 2704-2712.

Menzies, J., 2000. Micromorphological analyses of microfabrics and microstructures indicative of deformation processes in glacial sediments. Geological Society, London, Special Publications 176, 245-257.

Moon, T., Joughin, I., Smith, B., Broeke, M.R., Berg, W.J., Noël, B., Usher, M., 2014. Distinct patterns of seasonal Greenland glacier velocity. Geophysical Research Letters 41, 7209-7216.

Moran, S.R., Clayton, L., Hooke, R.L., Fenton, M.M., Andriashek, L.D., 1980. Glacier-bed landforms of The Prairie region of North America. Journal of Glaciology 25, 457-476.

Neudorf, C.M., Brennand, T.A., Lian, O.B., 2013. Till-forming processes beneath parts of the Cordilleran Ice Sheet, British Columbia, Canada: macroscale and microscale evidence and a new statistical technique for analysing microstructure data. Boreas 42, 848-875.

Norddahl, H., Ingólfsson, Ó., 2015. Collapse of the Icelandic ice sheet controlled by sea-level rise? arktos 1, 13.

Norddahl, H., Ingólfsson, Ó., Pétursson, H., G., Hallsdóttir, M., 2008. Late Weichselian and Holocene environmental history of Iceland. Jökull 58, 343-364.

Patton, H., Hubbard, A., Bradwell, T., Schomacker, A., 2017. The configuration, sensitivity and rapid retreat of the Late Weichselian Icelandic ice sheet. Earth-Science Reviews 166, 223-245.

Pedersen, S.A.S., 1987. Comparative studies of gravity tectonics in Quaternary sediments and sedimentary rocks related to fold belts, in: Jones, M.E., Preston, R.M.F. (Eds.), Deformation of Sediments and Sedimentary Rocks. Geological Society Special Publication, pp. 165-180.

Pedersen, S.A.S., 2005. Structural analysis of the Rubjerg Knude Glaciotectonic Complex, Vendsyssel, northern Denmark, Geological Survey of Denmark and Greenland Bulletin 8.

Phillips, E., Cotterill, C., Johnson, K., Crombie, K., James, L., Carr, S., Ruiter, A., 2018. Large-scale glacitectonic deformation in response to active ice sheet retreat across Dogger Bank (southern central North Sea) during the Last Glacial Maximum. Quaternary Science Reviews 179, 24-47.

Phillips, E., Everest, J., Evans, D.J.A., Finlayson, A., Ewertowski, M., Guild, A., Jones, L., 2017. Concentrated, 'pulsed' axial glacier flow: structural glaciological evidence from Kvíárjökull in SE Iceland. Earth Surface Processes and Landforms 42, 1901-1922.

Phillips, E., Everest, J., Reeves, H., 2013a. Micromorphological evidence for subglacial multiphase sedimentation and deformation during overpressurized fluid flow associated with hydrofracturing. Boreas 42, 395-427.

Phillips, E., Lipka, E., van der Meer, J.J.M., 2013b. Micromorphological evidence of liquefaction, injection and sediment deposition during basal sliding of glaciers. Quaternary Science Reviews 81, 114-137.

Phillips, E., Merritt, J., 2008. Evidence for multiphase water-escape during rafting of shelly marine sediments at Clava, Inverness-shire, NE Scotland. Quaternary Science Reviews 27, 988-1011.

Phillips, E., Merritt, J., Auton, C., Golledge, N., 2007. Microstructures in subglacial and proglacial sediments: understanding faults, folds and fabrics, and the influence of water on the style of deformation. Quaternary Science Reviews 26, 1499-1528.

Phillips, E.R., Auton, C.A., 2000. Micromorphological evidence for polyphase deformation of glaciolacustrine sediments from Strathspey, Scotland. Geological Society, London, Special Publications 176, 279-292.

Phillips, E.R., Lee, J.R., 2011. Glacitectonics-Field Guide, in: Phillips, E.R., Lee, J.R., Evans, H.M. (Eds.), Description measurement and analysis of glacitectonically deformed sequences. Quaternary Research Association.

Piotrowski, J.A., Tulaczyk, S., 1999. Subglacial conditions under the last ice sheet in northwest Germany: ice-bed separation and enhanced basal sliding? Quaternary Science Reviews 18, 737-751.

Ravier, E., Buoncristiani, J.-F., Menzies, J., Guiraud, M., Portier, E., 2015. Clastic injection dynamics during ice front oscillations: A case example from Sólheimajökull (Iceland). Sedimentary Geology 323, 92-109.

Rijsdijk, K.F., Owen, G., Warren, W.P., McCarroll, D., van der Meer, J.J.M., 1999. Clastic dykes in over-consolidated tills: evidence for subglacial hydrofracturing at Killiney Bay, eastern Ireland. Sedimentary Geology 129, 111-126.

Rotnicki, K., 1976. The theoretical basis for and a model of the origin of glaciotectonic deformations. Quaestiones Geographicae 3, 103-139.

Ruszczynska-Szenajch, H., 1987. The origin of glacial rafts: detachment, transport, deposition. Boreas 16, 101-112.

Rüther, D.C., Andreassen, K., Spagnolo, M., 2013. Aligned glaciotectonic rafts on the central Barents Sea seafloor revealing extensive glacitectonic erosion during the last deglaciation. Geophysical Research Letters 40, 6351-6355.

Sigfúsdóttir, T., Benediktsson, Í.Ö., Phillips, E., 2018. Active retreat of a Late Weichselian marine-terminating glacier: an example from Melasveit, western Iceland. Boreas 47, 813-836.

Sole, A.J., Mair, D.W.F., Nienow, P.W., Bartholomew, I.D., King, M.A., Burke, M.J., Joughin, I., 2011. Seasonal speedup of a Greenland marine-terminating outlet glacier forced by surface melt–induced changes in subglacial hydrology. Journal of Geophysical Research: Earth Surface 116.

Syvitski, J.P., Jennings, A.E., Andrews, J.T., 1999. High-resolution Seismic Evidence for Multiple Glaciation across the Southwest Iceland Shelf. Arctic, Antarctic, and Alpine Research 31, 50-57.

van der Meer, J.J.M., 1987. Micromorphology of glacial sediments as a tool in distinguishing genetic varieties of till. Geological Survey of Finland, Special Paper 3, 77-89.

van der Meer, J.J.M., 1993. Microscopic evidence of subglacial deformation. Quaternary Science Reviews 12, 553-587.

van Der Meer, J.J.M., Kjær, K.H., Krüger, J., 1999. Subglacial water-escape structures and till structures, Sléttjökull, Iceland. Journal of Quaternary Science 14, 191-205.

van der Meer, J.J.M., Kjær, K.H., Krüger, J., Rabassa, J., Kilfeather, A.A., 2009. Under pressure: clastic dykes in glacial settings. Quaternary Science Reviews 28, 708-720.

van der Wateren, D.F.M., 1985. A model of glacial tectonics, applied to the ice-pushed ridges in the Central Netherlands. Bull. geol. Soc. Denmark 34, 55-74.

van der Wateren, D.F.M., 1995. Structural geology and sedimentology of push moraines: processes of soft sediment deformation in a glacial environment and the distribution of glaciotectonic styles. Medelingen Rijks Geologische Dienst 54.

Vaughan-Hirsch, D.P., Phillips, E., Lee, J.R., Hart, J.K., 2013. Micromorphological analysis of poly-phase deformation associated with the transport and emplacement of glaciotectonic rafts at West Runton, north Norfolk, UK. Boreas 42, 376-394.

Vaughan-Hirsch, D.P., Phillips, E.R., 2017. Mid-Pleistocene thin-skinned glaciotectonic thrusting of the Aberdeen Ground Formation, Central Graben region, central North Sea. Journal of Quaternary Science 32, 196-212.

FIGURES

Figure 1. (a) The location of the Melasveit study area (black box) in western Iceland. The arrow indicates the ice flow into the area during the Late Weichselian. (b) A digital elevation model (Arctic DEM) of Melasveit. Thin black line represents the present coastline and the thick black lines denote the Melabakkar-Ásbakkar coastal cliffs. The red lines indicate the Melaleiti and Ásgil thrust-block moraines that are exposed in the cliffs. The curved, black solid line indicates the maximum extent of the Late Weichselian glacier advance from the north based on the configuration of the Skorholtsmelar end moraine. The dashed lines are an interpretation of the ice margin during different stages of a stepwise retreat, based on the location of buried moraines exposed in the coastal sections. (c) A photograph of the coastal section at Melaleiti. (d) A photograph of the coastal section at Ásgil. The moraine is exposed to the north (left side) of the ravine while associated submarine fan and overlying glaciomarine sediments are exposed on the southern side (right side) of the ravine.

Figure 2. (a) A scale diagram and a LiDAR scan of the Ásgil thrust-block moraine and overlying deposits (modified from Sigfúsdóttir et al., 2018). The red boxes indicate the sample locations and the area covered by Figs. 3-5. The black boxes mark the locations of photographs b-d. The photographs show the detachment separating the thrust-block from the footwall sand and gravel below. (b) A photo of the basal detachment at southern part of

the Ásgil moraine. The deformation is focused within a ~50 cm thick zone at the base of the thrust-block while the underlying deposits are largely undeformed (unit B). (c) A photo taken at ~2570 showing elongated intraclasts (dashed outlines) within fluidised sand at the base of the thrust-block. Hydrofractures infilled by coarse sands extend upwards and dissect the overlying thrust-block. (d) A photo taken at ~2520 m. The lower boundaries of the thrust-block are diffused and deformed by folds and faults. A ~10 m high and 2 m thick clastic breccia extends upwards into the thrust-blocks, an evidence of high water pressures.

Figure 3. (a) A section drawing showing the part of the detachment where samples Ásgil 1-5 were collected. The location is marked on Fig. 2a. (b) A photograph of the part of the detachment where samples Ásgil 2, 4 and 5 were collected. (c) A photograph of locations of samples Ásgil 5. Note a trowel for scale.

Figure 4. (a) A diagram showing the details of the basal detachment where samples Ásgil 6-8 were collected. The sample location is marked in Fig. 2a. Note that this is a less detailed diagram than Fig. 3. (b) A photograph of the sampling location.

Figure 5. (a) A diagram showing the basal detachment where samples Ásgil 9 and 10 were collected. The sample location is marked on Fig. 2a. Note that this is a less detailed diagram than Fig. 3. (b) A photograph of the sampling location.

Figure 6. Interpretation diagrams and scans of thin sections Ásgil 1-5. These thin sections were collected from a deformed zone at the base of the lowermost thrust-block, close to the leading edge of the Ásgil moraine. Their relative location can be seen on Fig. 3. These thin sections are dominated by layered, fine-grained sediments that have undergone repeated phases of sediment liquefaction, injection and hydrofracturing. Samples Ásgil 4 (a),

Ásgil 2 (b) and Ásgil 3 (c) are characterised by hydrofractures formed sub-parallel to the stratification of the fine-grained host deposits. Sample Ásgil 1(d) shows the margins of a steep, breccia filled hydrofracture (d). Sample Ásgil 5 (e) shows the infilling of a subhorizontal, breccia filled hydrofracture.

Figure 7. Interpretation diagrams and scans of thin sections Ásgil 8 (a) and Ásgil 10 (b). These thin sections were sampled from the base of the lowermost thrust block at a structurally deeper part of the moraine. The location of the thin sections can be seen on Figs. 4 and 5. They reveal fine grain, stratified sediments that have undergone alternating phases of shearing (folding, faulting) and hydrofracturing.

Figure 8. Interpretation diagram and scans of samples Ásgil 6 (a) and Ásgil 7 (b). These thin sections were sampled from the base of the lowermost thrust block at a structurally deeper part of the moraine. The locations of the thin sections can be seen in Fig. 3-4. These thin section were sampled from large hydrofractures dissecting the fine-grained sediment forming the thrust-block

Figure 9. (a) A scale diagram and a LiDAR scan of the Melaleiti thrust-block moraine (modified from Sigfúsdóttir et al., 2018). The red box indicates the sample locations and the area covered by Fig. 10. The black boxes on the LiDAR scan indicate the locations of photos b-d. The numbers on the section diagram indicate different thrust-blocks. (b) A photograph taken at ~140 m showing sharp lower contact (white dashed line) between a thrust-block above and the deformed silt and sand below. (c) A photograph taken at ~220 m showing faults dissecting the intrabedded silt and sand and the thrust-block above. The large normal fault seen in the middle part of the photo is infilled by massive sand (d) A close-up

photograph of the sediment-filled normal fault (hydrofracture) on Fig. c. The yellow scale is about 30 cm.

Figure 10. (a) A diagram showing the part of the basal detachment where samples Mel 11 - 16 were collected. The location is marked on Fig. 9a. (b) A photograph of the sampling location.

Figure 11. Interpretation diagram of samples Mel 16 (a), Mel 14 (b) and Mel 11 (c) The samples were collected from bedded/laminated glaciomarine sand and silt/clay located below the thrust-block detachment. The sampling locations are marked on Figure 10. These thin sections reveal that the folded interlaminated sediments are cross-cut by hydrofractures and faults/shears.

Figure 12. A sequential model explaining the formation of the moraines. See text for detailed description. Stage 1: As the glacier advanced across the sea-floor water pressures rose within the marine sediments. Porewater pressures build up within silt sand layers sealed between less permeable deposits. This caused liquifaction of the silt and sand enabling large sediment blocks to decouple from the underling sediments/or bedrock. Stage 2. The sediment blocks were transported forward do to gravity spreading and ice-push. Repeated phases of sediment liquifaction and injection occured along the earlier developed detahcment resulting in formation of complex hydrofracture system along the base of the sediment-blocks. The deformation associated with the tranport was focused within this realtive thin, water lubricated zone. Stage 3. The dislocated thrust-blocks were stacked at the ice-margins to form thrust-block moraines. The thrust-blocks were accreated on top of highly-permeable deposits of sands and gravels. Initially the thrust-blocks slid over the water-saturated sands and gravels without much internal deformation but with increased

sediment draining and elevated overburden pressures the friction increased. This resulted in folding and faulting separated by events of hydrofracturing and water escape. Stage 4. Further draining of the sediments lead to brittle deformation (faulting) and lock-up of the thrust blocks. Stage 5. The thrust-block moraine at Melaleiti was overriden. Water flowing under the base of the glacier resulted in deposition of coarse gravel and eroded the uppermost part of the moraine (Sigfúsdóttir et al., 2018). The Ásgil moraine shows no signs of having been overridden.

Supplementary Figure 1. Interpretation diagram and scan of sample Ásgil 9. This thin section was sampled from the lowermost thrust block at a structurally deeper part of the moraine. The location of the thin sections can be seen in Fig. 4.

Supplementary Figure 2. Interpretation diagrams and scans of samples Mel 12 (a), Mel 13 (b) and Mel 15 (c). The samples were collected from bedded/laminated glaciomarine sand and silt/clay located below the thrust-block detachment. The sampling locations are marked on Figure 10. These thin sections reveal that the sand underwent fluidisation causing brecciation of the clay-rich laminae. The sand is folded and the vergence of folds record apparent sense of shearing towards the southeast.

Figure 1

Click here to access/download;Figure;Fig1_Melasveit_map-01.tif

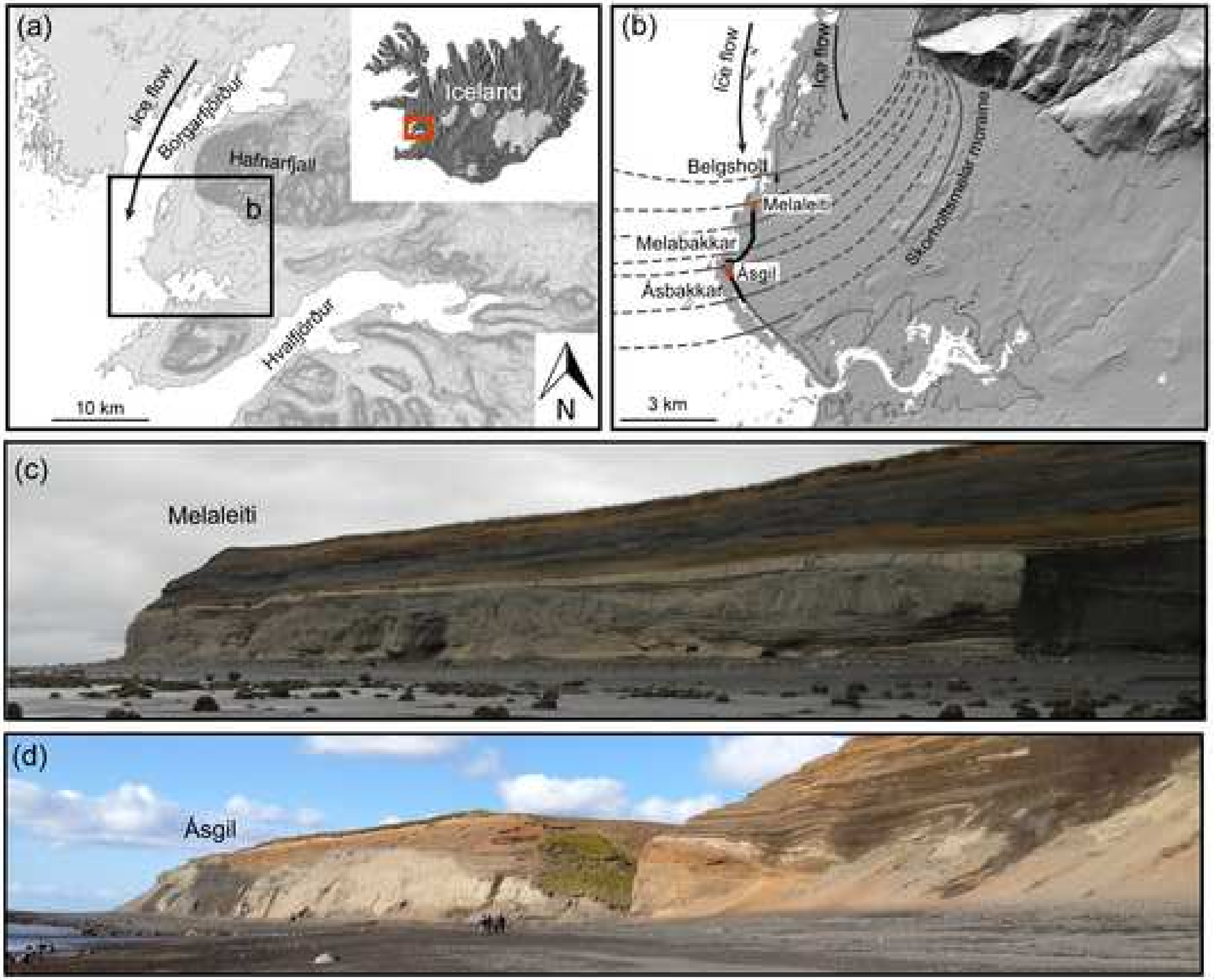

Figure 2

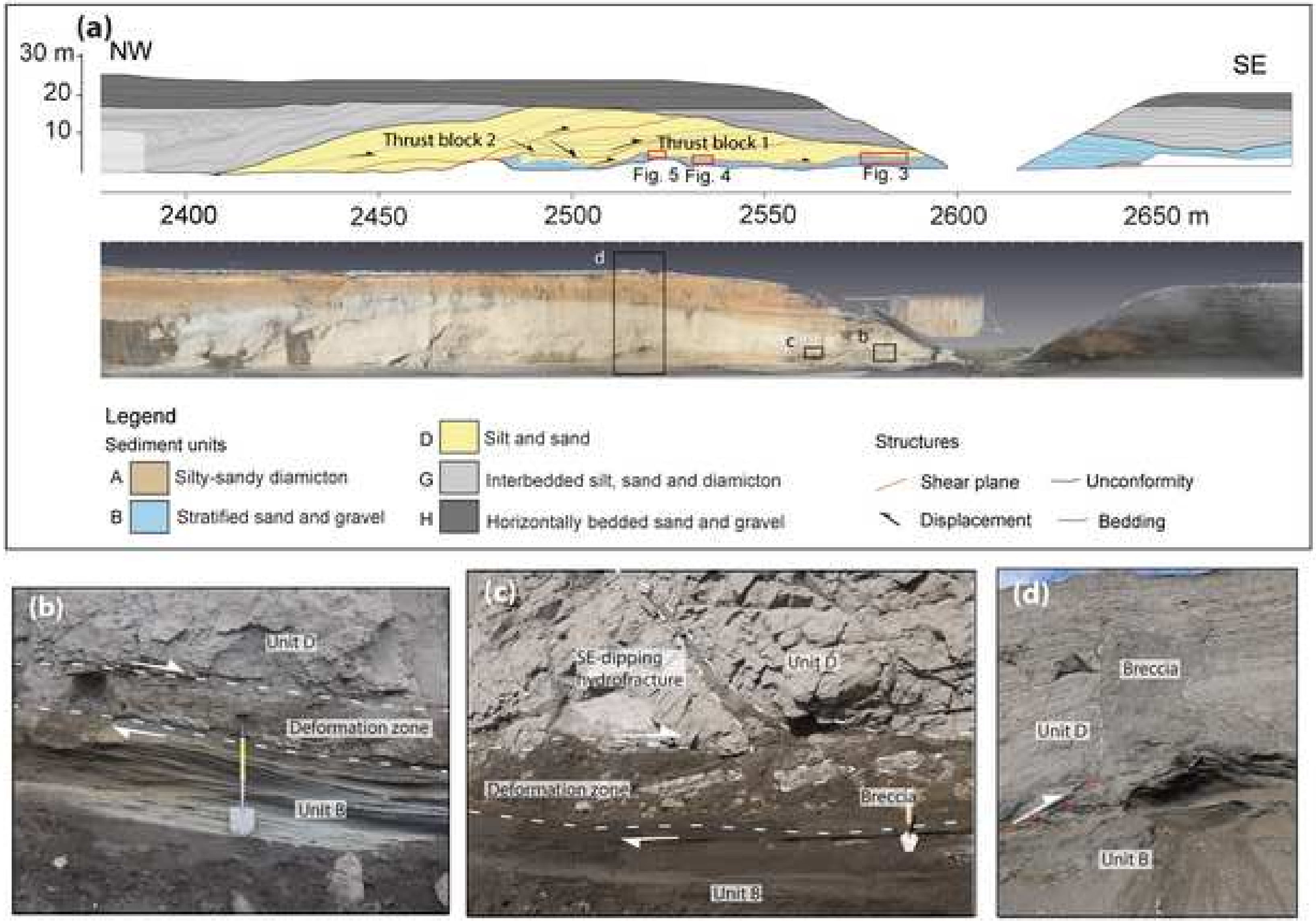
(a)
30 m
20
10
NW
SE
Thrust block 2
Thrust block 1
Fig. 5 Fig. 4
Fig. 3
2400
2450
2500
2550
2600
2650 m
d
c
b
Legend
Sediment units
A Silty-sandy diamicton
B Stratified sand and gravel
D Silt and sand
G Interbedded silt, sand and diamicton
H Horizontally bedded sand and gravel
Structures
Shear plane
Unconformity
Displacement
Bedding
(b)
Unit D
Deformation zone
Unit B
(c)
SE-dipping hydrofracture
Unit D
Deformation zone
Breccia
Unit B
(d)
Breccia
Unit D
Unit B

Figure 3

Click here to access/download;Figure;Fig3_Asgil_1_5-01.tif

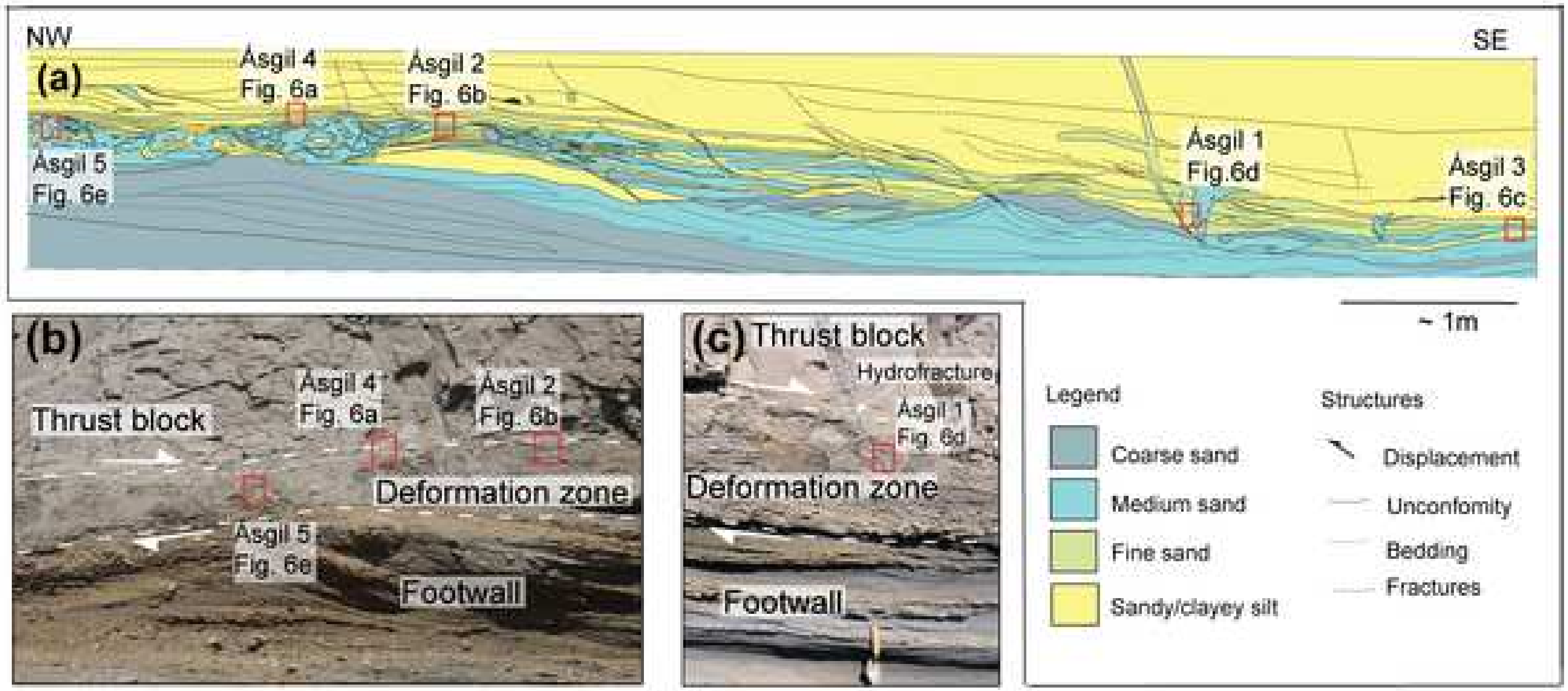

Figure 4

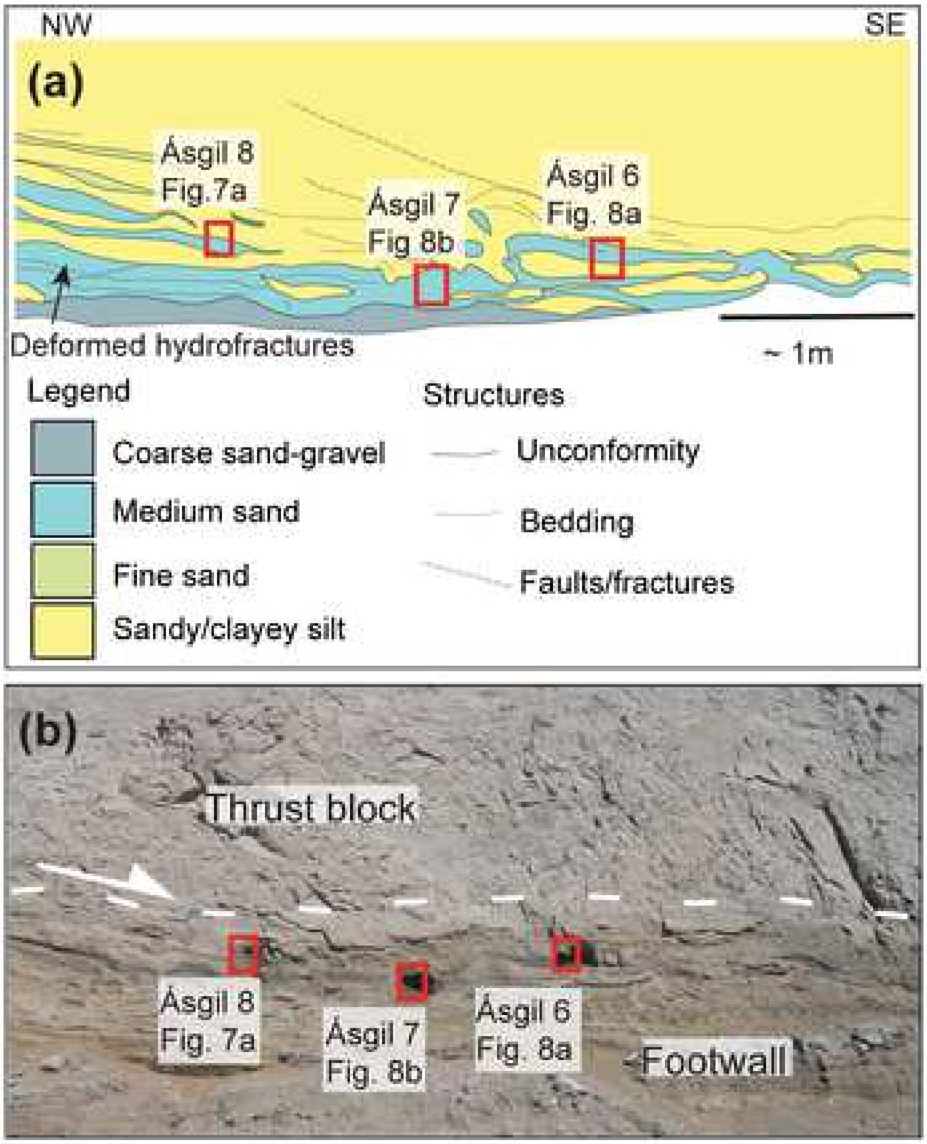
NW
SE
(a)
Ásgil 8
Fig.7a
Ásgil 7
Fig 8b
Ásgil 6
Fig. 8a
Deformed hydrofractures
~ 1m
Legend
Coarse sand-gravel
Medium sand
Fine sand
Sandy/clayey silt
Structures
Unconformity
Bedding
Faults/fractures
(b)
Thrust block
Ásgil 8
Fig. 7a
Ásgil 7
Fig. 8b
Ásgil 6
Fig. 8a
Footwall

Figure 5

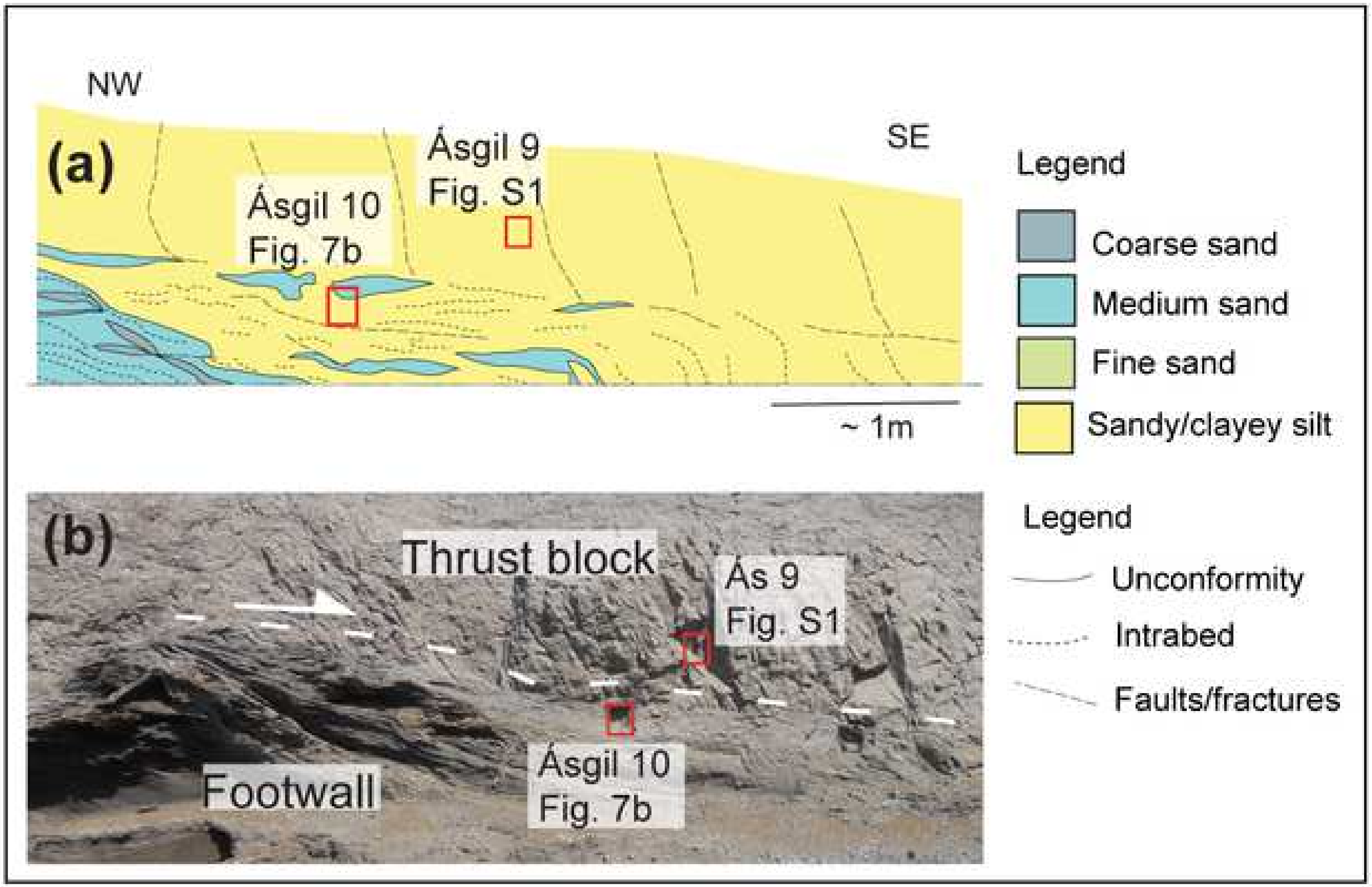
NW
(a)
Ásgil 10
Fig. 7b
Ásgil 9
Fig. S1
SE
~ 1m
Legend
Coarse sand
Medium sand
Fine sand
Sandy/clayey silt
(b)
Thrust block
Ás 9
Fig. S1
Footwall
Ásgil 10
Fig. 7b
Legend
Unconformity
Intrabed
Faults/fractures

Figure 6a

Click here to access/download;Figure;Fig6a_Thinsections1_5.tif

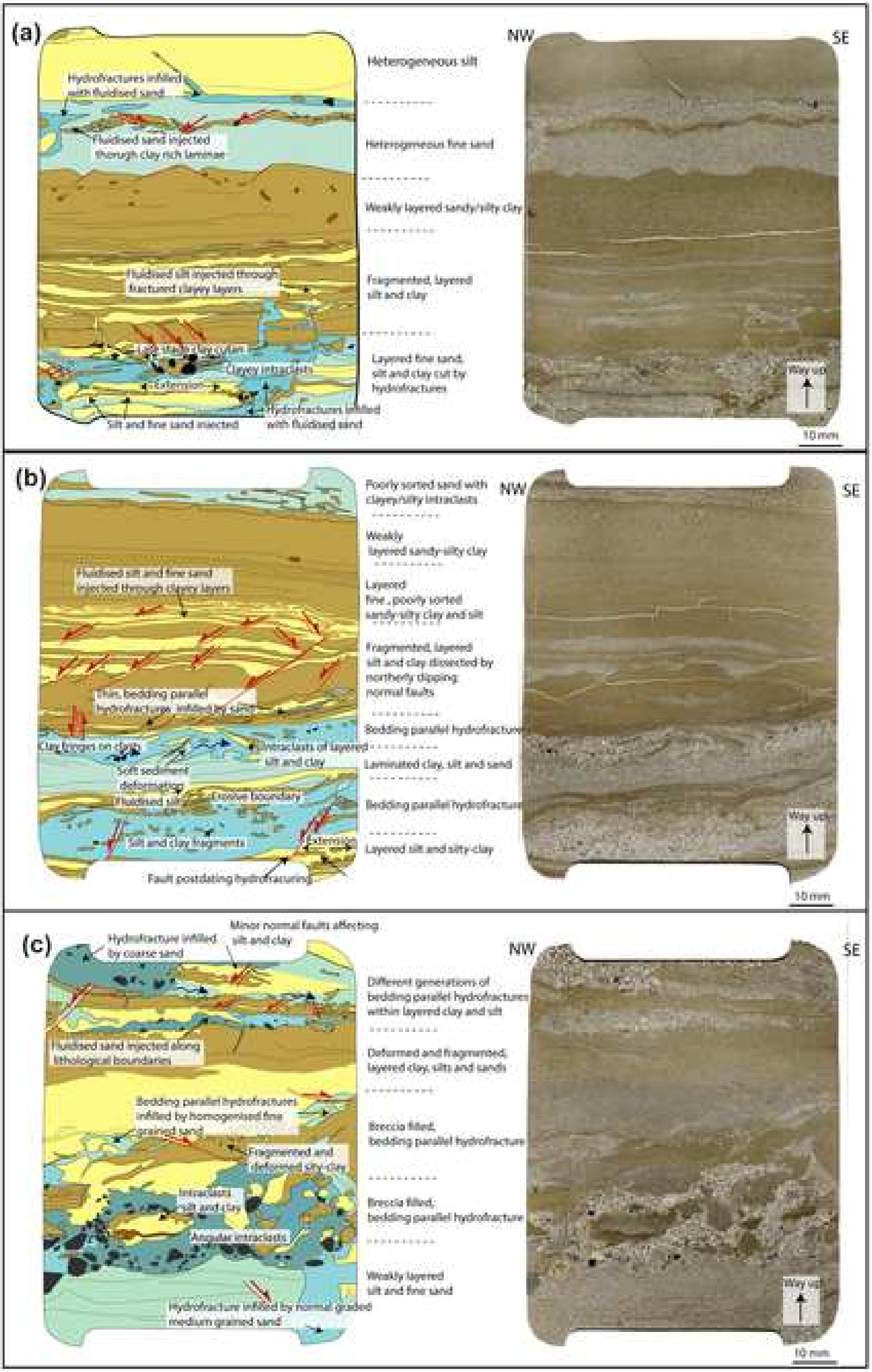

Figure 6b

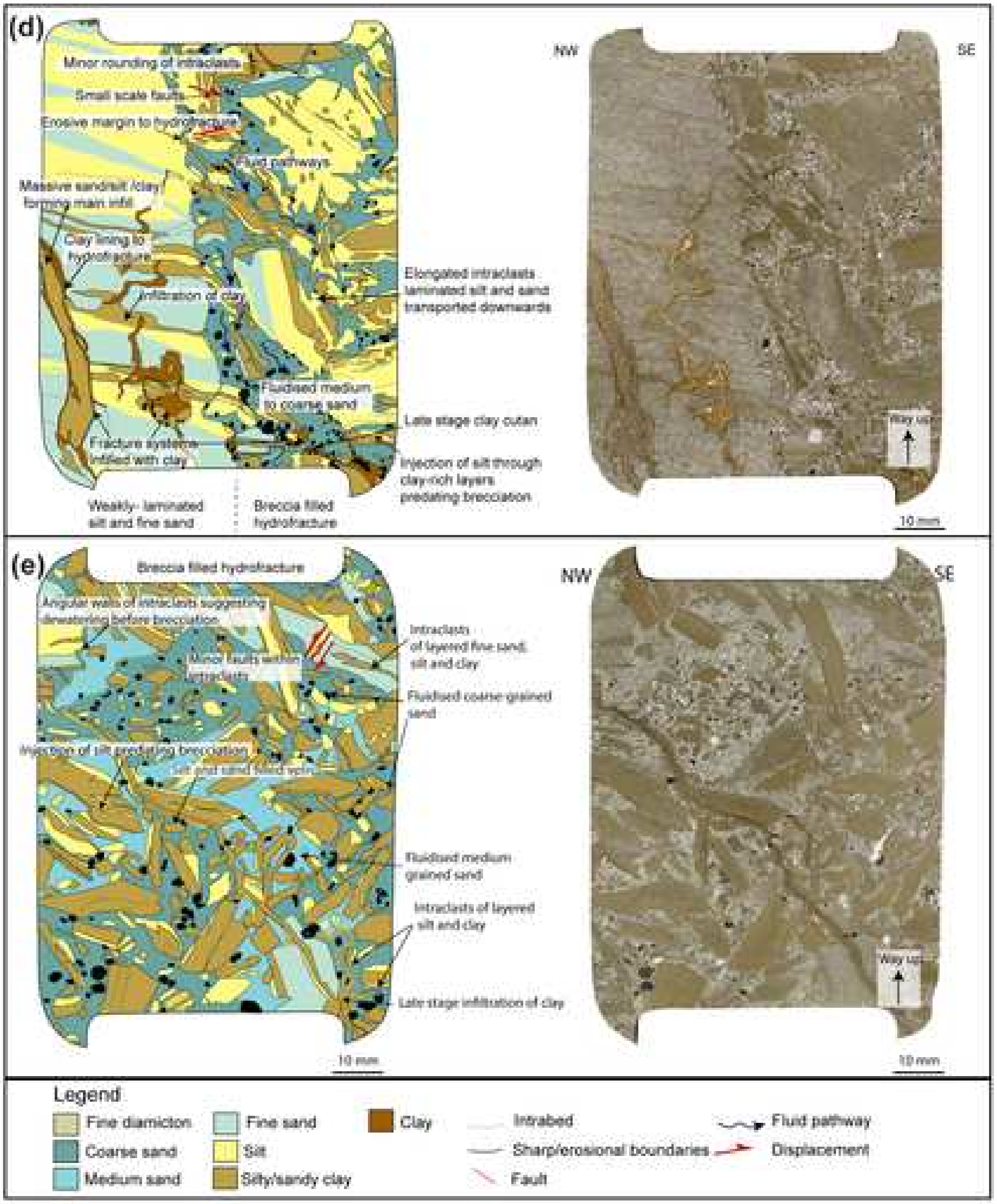
(d)
Minor rounding of intraclasts
Small scale faults
Erosive margin to hydrofracture
Fluid pathways
Massive sand/silt /clay forming main infill
Clay lining to hydrofracture
Infiltration of clay
Elongated intraclasts laminated silt and sand transported downwards
Fluidised medium to coarse sand
Late stage clay cutan
Fracture systems infilled with clay
Injection of silt through clay-rich layers predating brecciation
Weakly- laminated silt and fine sand
Breccia filled hydrofracture
NW
SE
Way up
10 mm
(e)
Breccia filled hydrofracture
Angular walls of intraclasts suggesting dewatering before brecciation
Minor faults within intraclasts
Intraclasts of layered fine sand, silt and clay
Fluidised coarse grained sand
Injection of silt predating brecciation
Silt and sand filled vein
Fluidised medium grained sand
Intraclasts of layered silt and clay
Late stage infiltration of clay
NW
SE
Way up
10 mm
10 mm
Legend
Fine diamicton
Coarse sand
Medium sand
Fine sand
Silt
Silty/sandy clay
Clay
Intrabed
Sharp/erosional boundaries
Fault
Fluid pathway
Displacement

Figure 7

Click here to access/download;Figure;Fig7_Thinsections8_10.tif

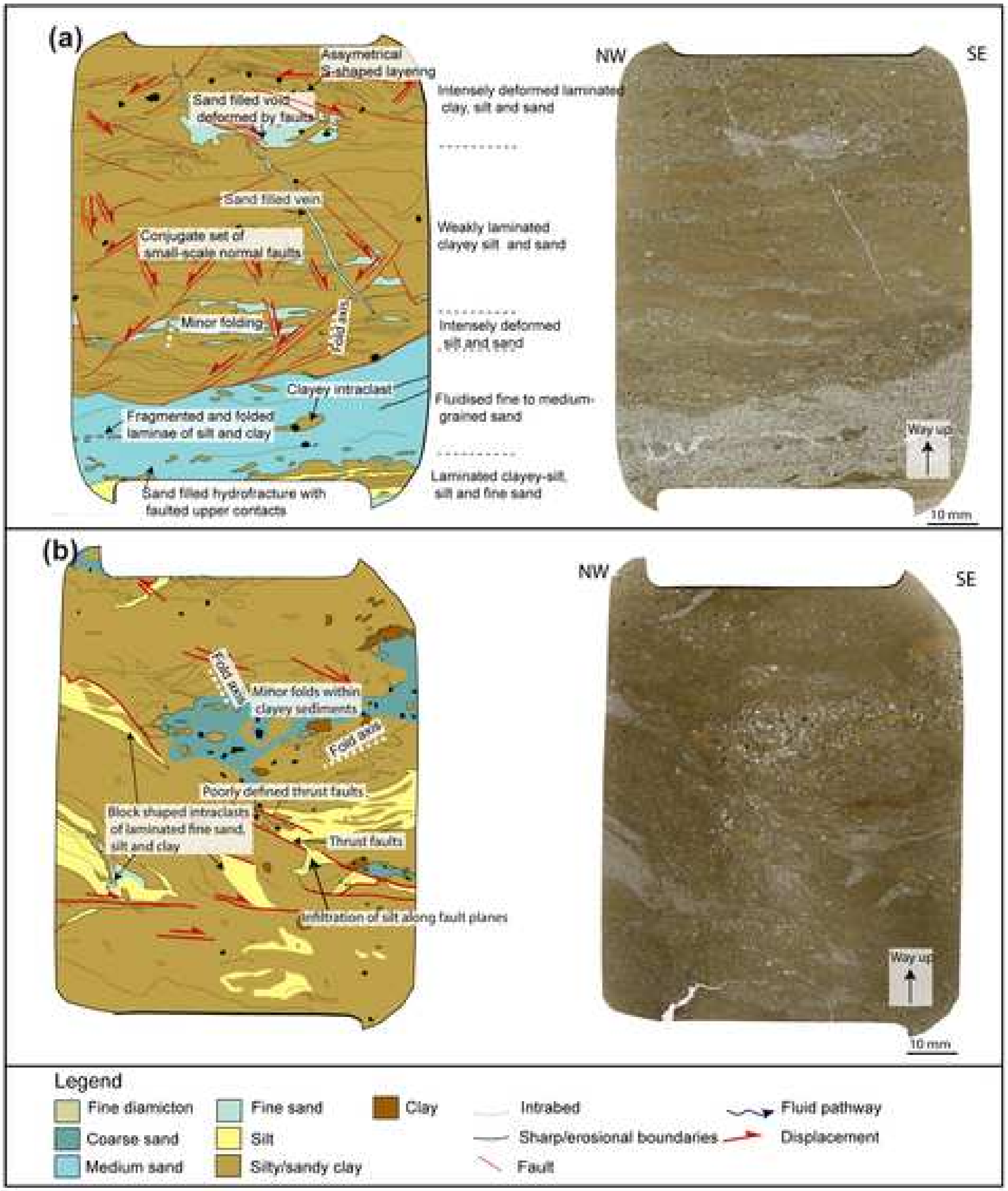

Figure 8

Click here to access/download;Figure;Fig8_Thinsections_6_7.tif

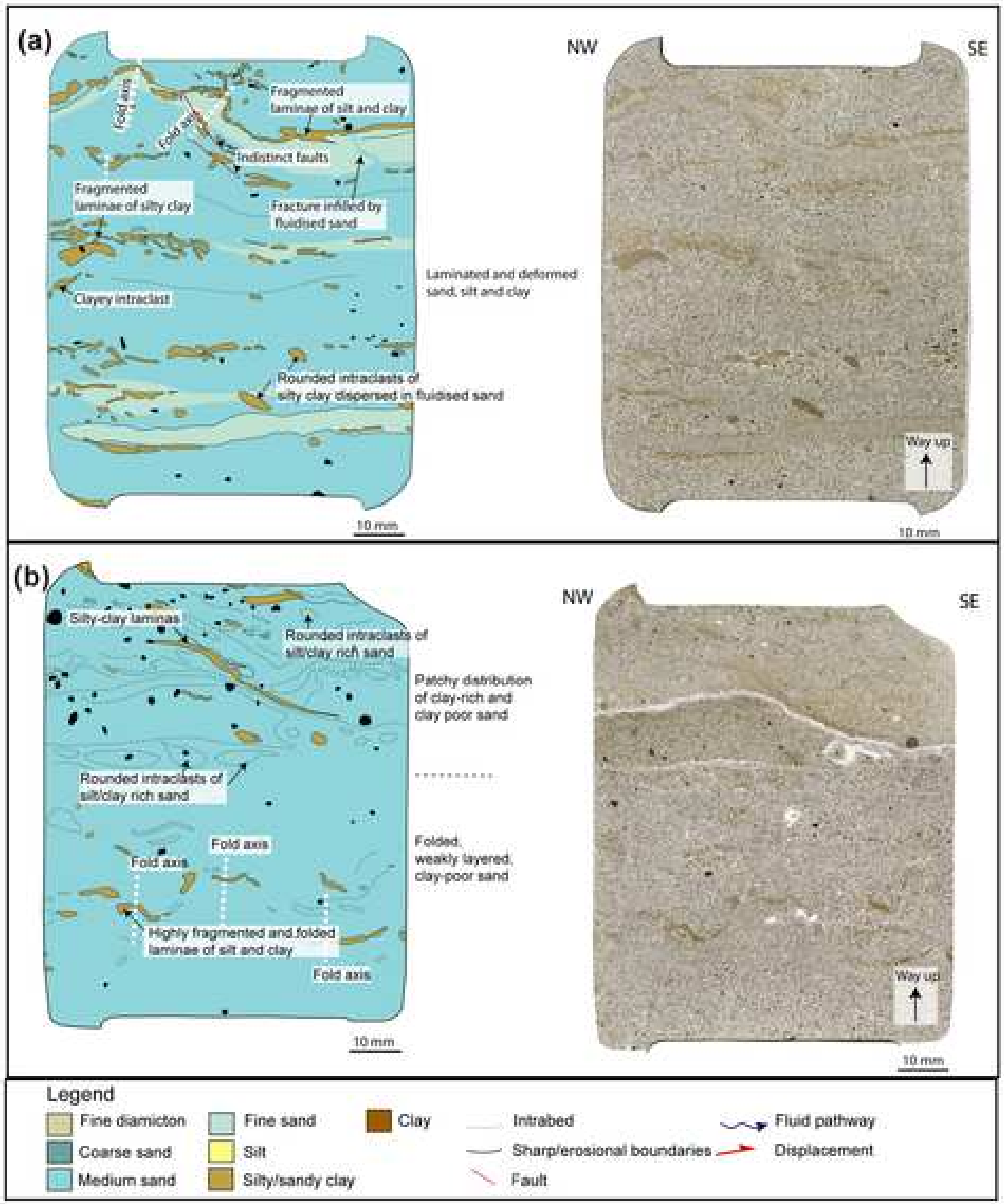

Figure 9

Click here to access/download;Figure;Fig9_Melaleiti.tif

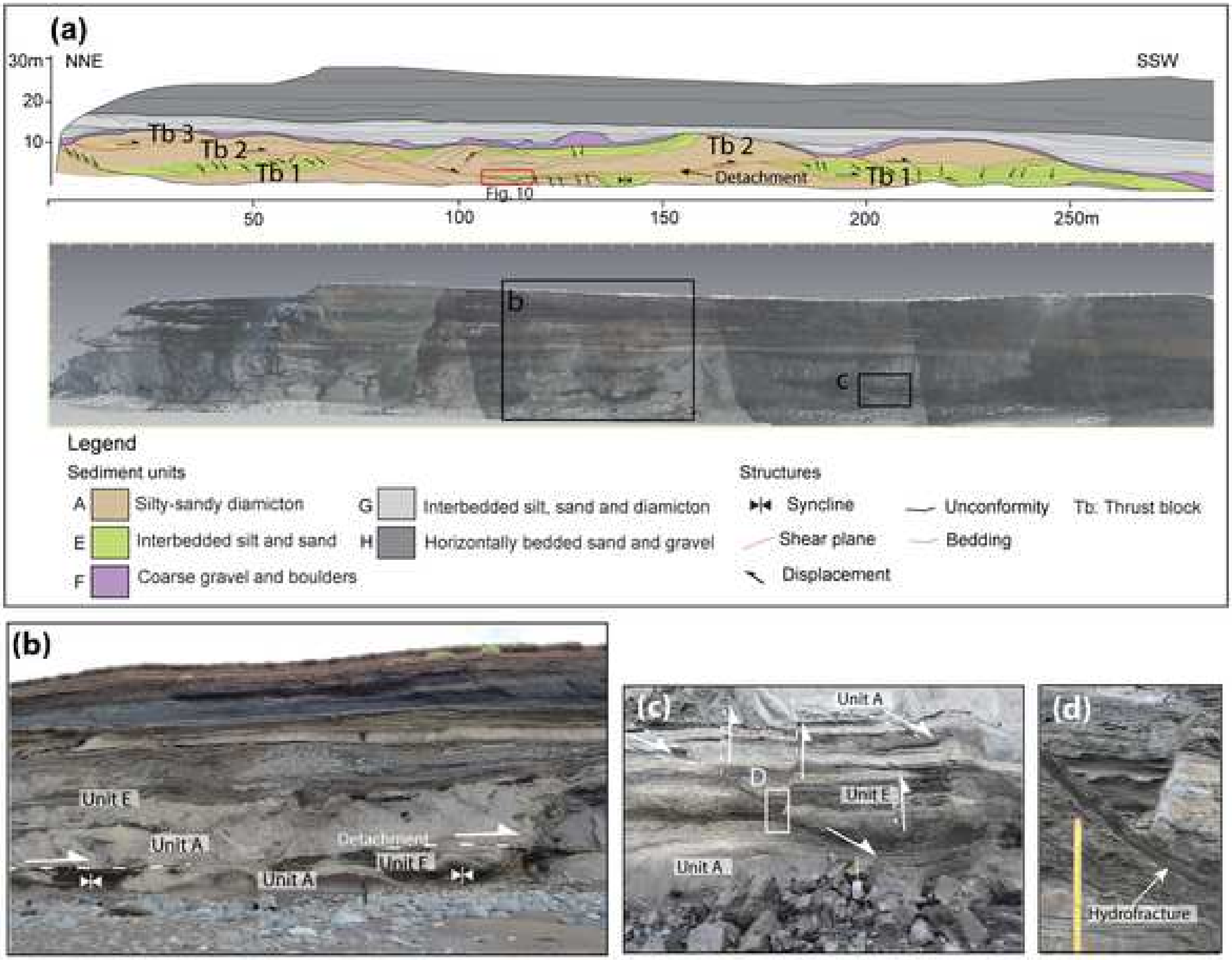

Figure 10

Click here to access/download;Figure;Fig10_Thinsections_11-16_location-01.tif

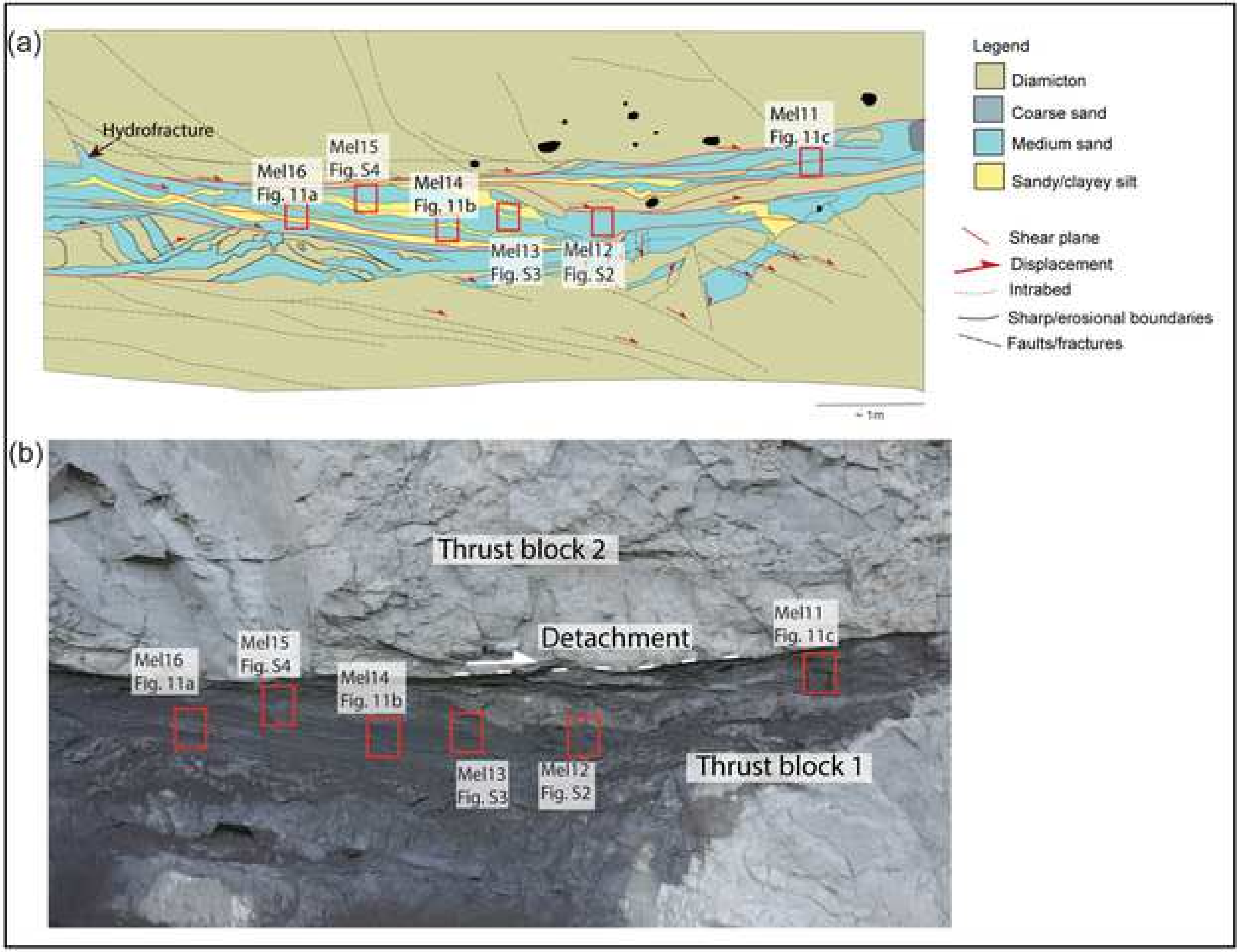

Figure 11

Click here to access/download;Figure;Fig11_Thinsections_11_14_16.tif

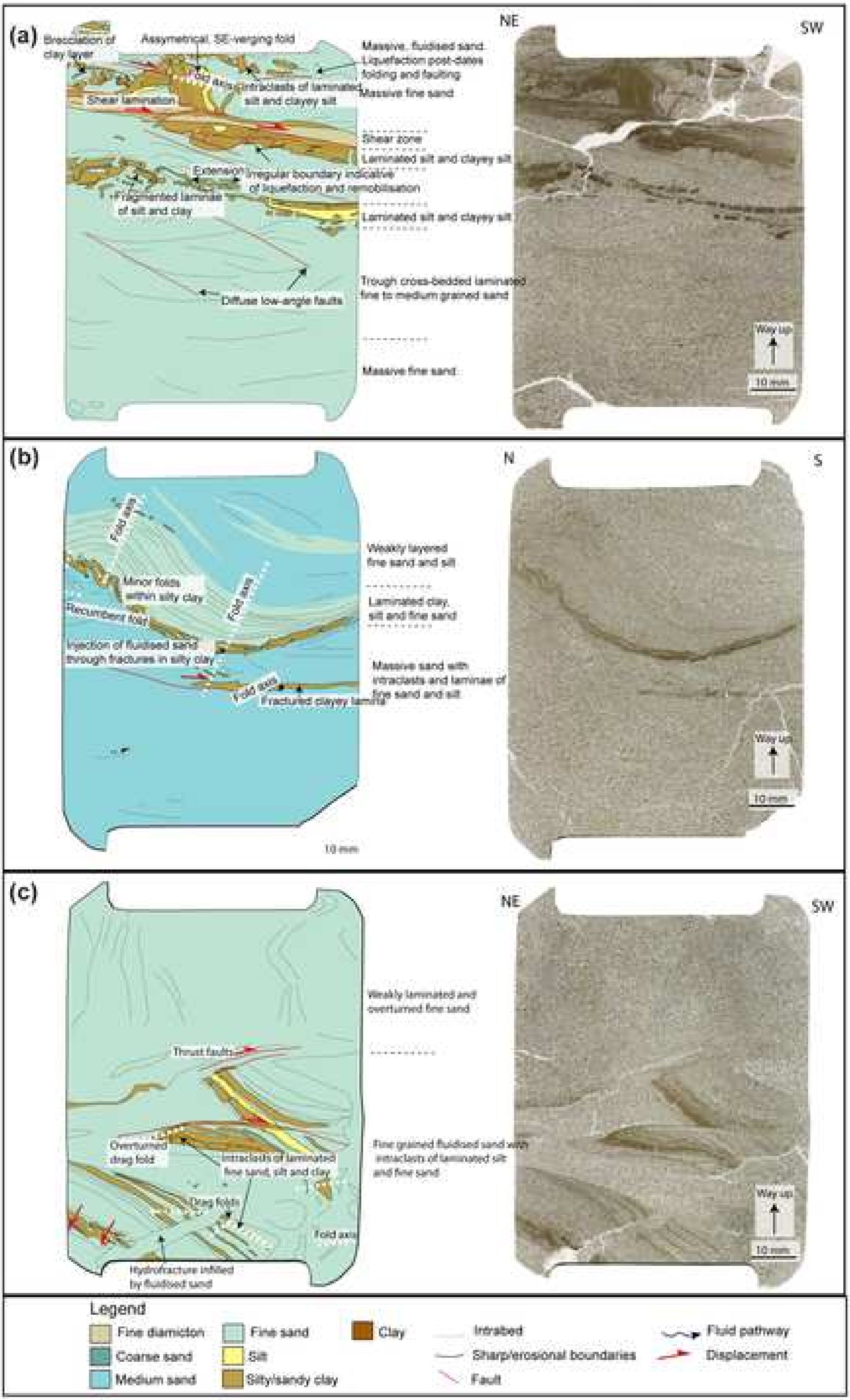

Figure 12

Click here to access/download;Figure;Fig12_model-01.tif

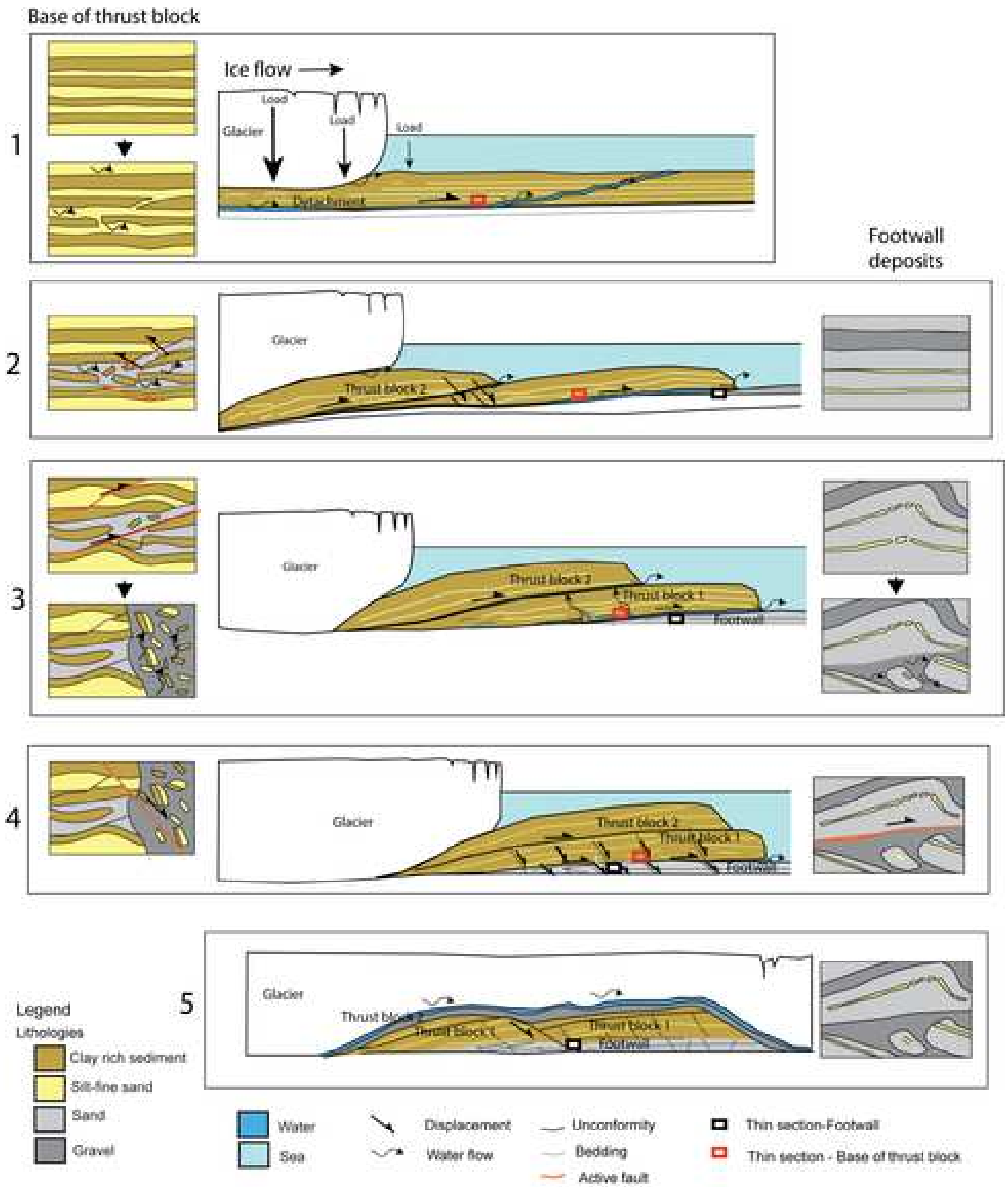

Figure S1

Click here to access/download;Supplemental Material (Online Only);FigS1_Raft9_micro.tif

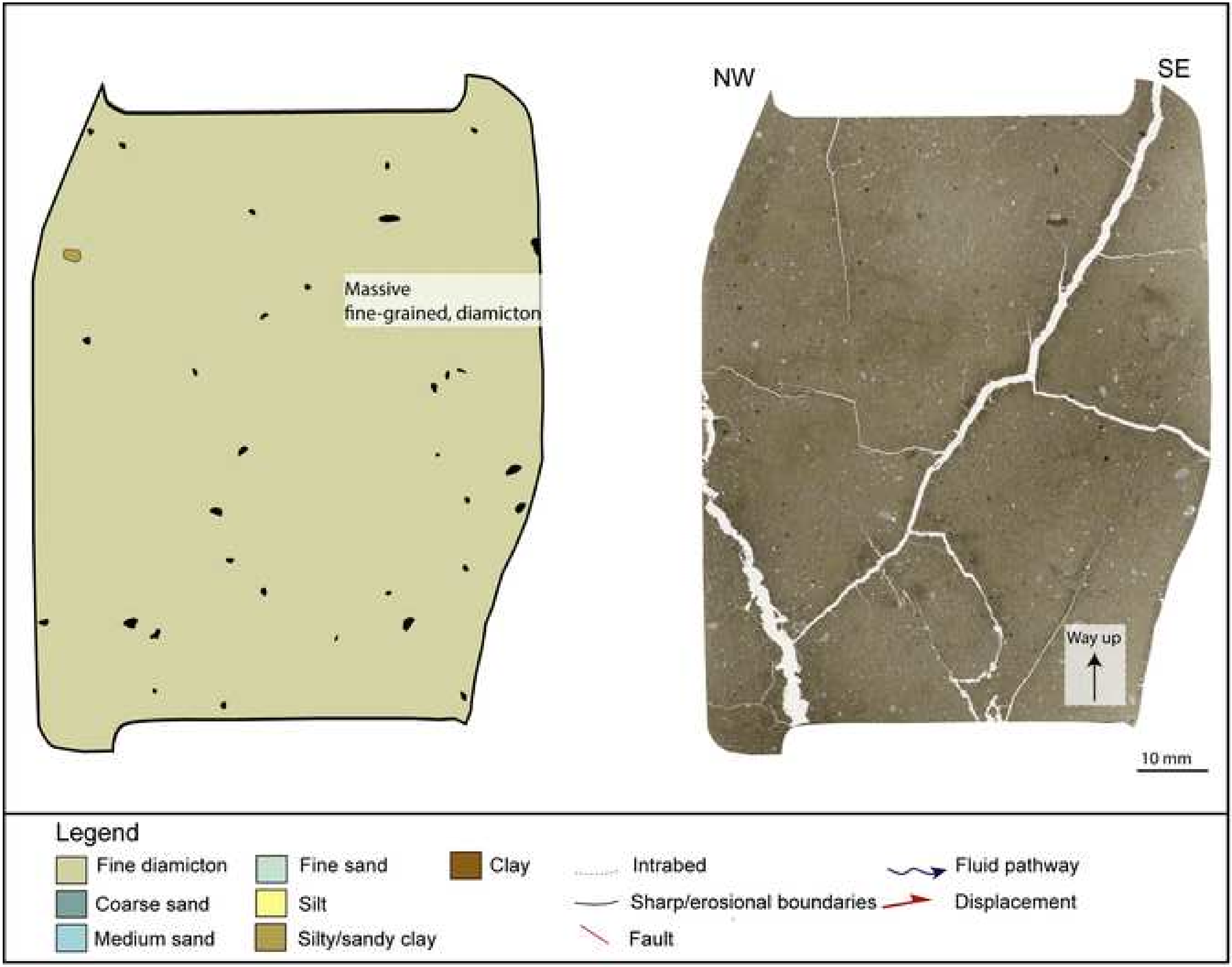

Figure S2

Click here to access/download;Supplemental Material (Online Only);FigS2_thinsections_12_13_15.tif